Eur. Phys. J. C 54, 601–616 (2008)
DOI 10.1140/epjc/s10052-008-0546-1

THE EUROPEAN PHYSICAL JOURNAL C

Regular Article – Theoretical Physics

MSSM Higgs sector CP violation at photon colliders: revisited

Saebyok Bae[1,a], Byungchul Chung[2,b], P. Ko[3,c]

[1] Institute for Gifted Students, KAIST, 335 Gwahangno, Yuseong-gu, Daejeon 305-701, South Korea
[2] Proton Engineering Frontier Project, KAERI, Daejeon 305-701, South Korea
[3] School of Physics, KIAS, Seoul 130-722, South Korea

Received: 22 August 2007 / Revised version: 8 November 2007 /
Published online: 28 February 2008 – © Springer-Verlag / Società Italiana di Fisica 2008

Abstract. The CP violating phases in soft SUSY breaking terms may induce indirect CP violation in the neutral Higgs boson sector through SUSY particle loops as well as direct CP violation in the $\gamma\gamma \to H_i$ $(i = 1, 2, 3)$ through CP violating vertices. We present a complete analysis of the MSSM Higgs sector CP violation at photon colliders including the chargino loop contributions in the regime $\tan\beta \lesssim 20$, where the CP violating mixing in the neutral Higgs sector is very strongly influenced by the scalar top loop, more so than the chargino and neutralino ones. However, the CP violating phases of the higgsino and wino mass parameters may still generate direct CP violation in $\gamma\gamma \to H_i$. In this process, the CP violating phenomena become very rich, and thus we study the production rates and polarization asymmetries in the Higgs production in detail. Photon colliders with high luminosity and well controlled polarized initial photon beams are indispensable in determining the CP properties of neutral Higgs bosons.

PACS. 14.80.Cp; 12.60.Jv; 11.30.Er

1 Introduction

The discovery of Higgs bosons at the current/future colliders is one of the most important goals of high energy particle physics experiments. Their (non-) discovery would be crucial for testing our present understanding of the origin of electroweak symmetry breaking and the subsequent generation of masses of electroweak gauge bosons and chiral fermions in the standard model (SM). This would be also true of the minimal supersymmetric standard model (MSSM), which is the most popular candidate for new physics beyond the SM.

The Higgs sector in the MSSM possesses three neutral Higgs particles: two CP even neutral scalars (h and H), one CP odd neutral scalar (A) in the CP conserving limit, and a pair of charged Higgs scalars ($H^{\pm}$) [1]. The tree-level MSSM Higgs potential does not allow spontaneous CP violation unlike general two-Higgs doublet model. Even if one would include the one-loop corrected effective potential for the Higgs sector, spontaneous CP violation [2] cannot be realistic, because the resulting lightest neutral Higgs boson should be far lighter than the current lower limit on the Higgs boson mass [3–5]. Still, there are many new explicitly CP violating complex parameters in the soft supersymmetry (SUSY) breaking sector of the MSSM Lagrangian. Some complex parameters may have large phases without any conflict with the electron/neutron electric dipole moment (EDM) constraints. Then, these phases can lead to some observable consequences in various CP violating phenomena in K and B decays [6] and electroweak baryogenesis [7–10], etc. Especially, the complex phases of the stop and sbottom trilinear couplings $A_{t,b}$ and the higgsino mass parameter μ may cause mixing between CP odd and CP even Higgs bosons in the neutral Higgs sector via loop corrections in the MSSM, i.e., the Higgs sector CP violation [11–13].

In most phenomenological studies of the MSSM, the large SUSY CP violating (CPV) phases were usually neglected, since they may lead to too large EDMs of electron and neutron, or ϵ_K, depending on whether they are flavor preserving or flavor changing. The simplest way to evade the EDM constraints is to assume that SUSY CPV phases are vanishingly small. Thus, the only source of CP violation would be the single Kobayashi–Maskawa (KM) phase in the CKM mixing matrix in the charged weak current of down type quarks. In this case, the SUSY effects on K and B phenomenology are minimal in the sense that deviations from the SM predictions are quite small. However, one can still consider large FP SUSY CPV phases, since the EDM constraints can be avoided in various manners.

- Decoupling (effective SUSY model): the first/second generation sfermions are heavy (and degenerate to some extent) enough, so that the SUSY CP and ϵ_K prob-

[a] e-mail: sbae@kaist.ac.kr
[b] e-mail: cbc0726@kaeri.re.kr
[c] e-mail: pko@kias.re.kr

lems are evaded. Only the third generation sfermions and gauginos have to be lighter than $O(1)$ TeV in order to solve the gauge hierarchy problem by SUSY [14–17]. In this case, the SUSY CPV phases need not be zero, and they may lead to substantial deviations from the SM cases, especially for the third generation. In this scenario, B factories may be able to probe the SUSY CPV phases from direct asymmetry in $B \to X_s\gamma$ and the lepton forward–backward asymmetry in $B \to X_s l^+ l^-$, etc.
- Cancellation: various contributions to electron/neutron EDMs may cancel one another, leading to net results that are consistent with experimental lower bounds [18–21]. In this case, many of the SUSY CPV phases may be $O(1)$ as in the decoupling scenario. However, this scenario is tightly constrained when the data on the mercury (^{199}Hg) atom EDM are included [22, 23].
- Non-universal scenario: the absolute values $|A_e|$, $|A_{u,c}|$, $|A_{d,s}| \lesssim 10^{-3}|\mu|$ evade e/n EDM constraints, but $A_{t,b,\tau}$ can have large CP violating phases [24]. However, there is a strong two-loop Barr–Zee type constraint for large $\tan\beta$. Therefore, large CPV phases can be allowed in this scenario and the decoupling scenario only for $\tan\beta \lesssim 20$–30.

Assuming some SUSY CPV phases of about $O(1)$ without any conflict with the EDM constraints, it can be imagined that there could be CP violation in the neutral Higgs boson sector in the MSSM, which can be studied by observing the CP properties of all the three Higgs particles directly. Higgs bosons can be produced in $\gamma\gamma$ collisions via one-loop diagrams in which all the possible charged particles participate. The s-channel resonance productions of the neutral Higgs bosons in $\gamma\gamma$ collisions have been considered as crucial tools for studying the CP properties of the Higgs particles [25–28]. Because the polarizations of the colliding photons can strongly govern both the $\gamma\gamma$ luminosity spectrum and the cross sections, obtaining the highly polarized photon beams is important for Higgs boson detection. This can be realized by Compton backscattering of laser photons off the linear collider electron and positron beams, which can produce high luminosity $\gamma\gamma$ collisions with a wide spectrum of $\gamma\gamma$ center of mass energy [29–32]. In the meanwhile, related researches for photon collisions [33] are, for example, the effects of Higgs sector CP violation on the $t\bar{t}$ pair production [34], and the CP asymmetries [35] and fermion polarizations [36] in various fermion pair productions. In addition, there are also studies on the Higgs sector at various colliders such as the tevatron, the LHC, and the linear colliders [37–42].

In particular, one can observe the CP violating effects through the s-channel resonance for the neutral Higgs particle production at the linear collider in the $\gamma\gamma$ mode. Due to the mixing effect between the CP odd and CP even neutral Higgs bosons, the additional loops of charged scalars and vectors contribute to the production in the $\gamma\gamma$ collision of the would-be CP odd neutral Higgs H_2 (corresponding to the CP odd neutral Higgs A in the CP conserving limit), resulting in an enhanced production cross section. In [43, 44], CP violation of the neutral Higgs sector at a photon collider was studied using the s-channel resonance production cross sections and the polarization asymmetries of the Higgs particles for $3 \le \tan\beta \le 10$. In the loop diagrams relevant to $\gamma\gamma \to H_{i=1,2,3}$, the neutral Higgs bosons, chargino loop contributions were neglected by assuming that the charginos were heavy enough to be decoupled from the production of the Higgs bosons [43, 44]. In this work, we revisit the issue of CP violation at a photon collider including the chargino contributions, and study the CP properties of neutral Higgs bosons in the MSSM. In the meanwhile, the inclusion of the chargino loops in $\gamma\gamma \to H_i$ may be important for the following reasons.

- Since all the charged particles interacting with the neutral Higgs bosons will contribute to $\gamma\gamma \to H_i$, it is mandatory to include the chargino effects in a study of the neutral Higgs boson production at photon colliders.
- Especially, the charginos in the MSSM are not much heavier than the lighter stop in many SUSY breaking scenarios. The current lower limit on the lighter chargino mass from LEP II experiment is only $M_{\tilde{\chi}_1^-} > 103(83.6)$ GeV for $m_{\tilde{\nu}} > (<)$ 300 GeV in the minimal supergravity scenario [45]. In the AMSB scenario, it is even less stringent (i.e., $M_{\tilde{\chi}_1^-} > 45$ GeV). Thus, their effects should not be excluded in any realistic analysis. In this work, we have found that the chargino effects often dominate the stop loop contributions even in the CP conserving limit.
- If the chargino loops are included in the subject of CP violation in the neutral Higgs sector, it is natural to treat the M_2 and μ parameters in the chargino mass matrix as complex numbers. Then, this will open up a new possibility of direct CP violation in $\gamma\gamma \to H_i$, which is newly addressed in the present work. Although the complex phases in M_2 and μ may also contribute to the CP violating mixing among neutral Higgs bosons through chargino loops, such effects are not important for $\tan\beta \lesssim 20$. Since the CPV phases are strongly constrained in the large $\tan\beta$ region, it might be plausible to consider low or medium range of $\tan\beta$ up to 20. However, the LEP data of four collaborations [46] seem to exclude the small values of $\tan\beta \lesssim O(3)$ in the CP violating MSSM, and thus we will stick to $\tan\beta = 10$ in our numerical analysis. So, introducing the CP phases in the chargino sector will not induce an appreciable CP violation in the Higgs mixing. However, they can generate direct CP violation in the decay/production amplitudes for $\gamma\gamma \to H_i$. This is an entirely new CP violating phenomenon, which can occur by considering the chargino loop contributions to $\gamma\gamma \to H_i$.

This paper is organized as follows. In Sect. 2, we review briefly the loop-induced CP violation and the mixing of CP even and CP odd Higgs bosons in the neutral Higgs sector of the MSSM. In Sect. 3, we derive the cross sections for Higgs production in $\gamma\gamma$ collisions and the polarization asymmetries in terms of two form factors appearing in the $\gamma\gamma \to H_{i=1,2,3}$ amplitudes. In Sect. 4, we present detailed numerical analyses and discuss the potential importance of chargino loop contributions to the CP violation in the neutral Higgs production. The formulae for the chargino and

stop mass matrices, their eigenvalues and the corresponding mixing matrices are given in Appendix A. In addition, the interaction Lagrangian relevant to $\gamma\gamma \to H_i$ is recapitulated for both convenience and completeness.

2 The neutral Higgs sector in the MSSM

The MSSM Lagrangian possesses many new CP violating phases in the soft SUSY breaking terms in addition to the KM phase in the CKM matrix element. In the MSSM, the Higgs potential is CP conserving at the tree level, and only the soft terms (and the usual CKM mixing matrix) can have CP violating phases. We will work with the convention that the Higgs bilinear soft parameter $B\mu$ is set real by Peccei–Quinn $\mathrm{U(1)_{PQ}}$. However, the CPV phases in the soft terms can induce CP violation in the effective potential of the Higgs bosons through quantum corrections involving squarks and other SUSY particles in the loops. This phenomenon will lead to CP violating mixing between the would-be CP even (corresponding to h, H in the CP conserving limit) and the would-be CP odd (corresponding to A) Higgs fields.

The effective potential of the Higgs fields at the one-loop level can be written as

$$\begin{aligned}\mathcal{V}^{\mathrm{eff}}_{\mathrm{Higgs}} = {} & \mu_1^2\Phi_1^\dagger\Phi_1 + \mu_2^2\Phi_2^\dagger\Phi_2 + \left(m_{12}^2\Phi_1^\dagger\Phi_2 + \mathrm{h.c.}\right) \\ & + \lambda_1(\Phi_1^\dagger\Phi_1)^2 + \lambda_2(\Phi_2^\dagger\Phi_2)^2 + \lambda_3(\Phi_1^\dagger\Phi_1)(\Phi_2^\dagger\Phi_2) \\ & + \lambda_4(\Phi_1^\dagger\Phi_2)(\Phi_2^\dagger\Phi_1) + \lambda_5(\Phi_1^\dagger\Phi_2)^2 + \lambda_5^*(\Phi_2^\dagger\Phi_1)^2 \\ & + \lambda_6(\Phi_1^\dagger\Phi_1)(\Phi_1^\dagger\Phi_2) + \lambda_6^*(\Phi_1^\dagger\Phi_1)(\Phi_2^\dagger\Phi_1) \\ & + \lambda_7(\Phi_2^\dagger\Phi_2)(\Phi_1^\dagger\Phi_2) + \lambda_7^*(\Phi_2^\dagger\Phi_2)(\Phi_2^\dagger\Phi_1)\,, \end{aligned} \tag{1}$$

where $\tilde{\Phi}_1 = \mathrm{i}\tau_2\Phi_1^*$ (τ_2 is the Pauli matrix) is the scalar component of the Higgs superfield $\widehat{H}_1$ giving masses to down type fermions, and Φ_2 is the scalar component of $\widehat{H}_2$. At the tree level, the dimension-2 parameters and the quartic couplings are given by $\mu_a^2 = -m_a^2 - |\mu|^2$ ($a = 1, 2$) with soft Higgs masses m_a^2, $\lambda_1 = \lambda_2 = -\frac{1}{8}(g^2 + g'^2)$, $\lambda_3 = -\frac{1}{4}(g^2 - g'^2)$ and $\lambda_4 = \frac{1}{2}g^2$, respectively. Due to $\lambda_b = 0$ ($b = 5, 6, 7$) at the tree level, there is no Higgs sector CP violation in the MSSM at the tree level. However, nonzero values of $\lambda_{a=5,6,7}$ can be generated at the one-loop level, and they can be complex if soft SUSY breaking parameters like A_t, μ or M_2 have CPV phases. The heuristic explanation of this Higgs scalar–pseudoscalar mixing is given in the first paper of [47, 48] using a toy model. The analytic expressions including the loop corrections are presented in the first and third ones in [11–13].

Since the electroweak gauge symmetry is known to be broken spontaneously into $\mathrm{U(1)_{em}}$ in nature, the two Higgs doublets can be written as

$$\begin{aligned}\Phi_1 &= \begin{pmatrix} \phi_1^+ \\ (v_1 + \phi_1 + \mathrm{i}a_1)/\sqrt{2} \end{pmatrix}, \\ \Phi_2 &= \mathrm{e}^{\mathrm{i}\xi}\begin{pmatrix} \phi_2^+ \\ (v_2 + \phi_2 + \mathrm{i}a_2)/\sqrt{2} \end{pmatrix}, \end{aligned} \tag{2}$$

where the VEVs v_i are real. The relative phase ξ, which is renormalization-scheme dependent (see the third paper of [11–13]), is determined from the minimum energy conditions of the Higgs potential [11–13], i.e., the vanishing tadpole conditions $T_\phi = \partial\mathcal{V}^{\mathrm{eff}}_{\mathrm{Higgs}}/\partial\phi = 0$ ($\phi = \phi_1, \phi_2, a_1, a_2$). It turns out that ξ is very small in the $\overline{\mathrm{MS}}$ scheme, so it will be ignored in the numerical analysis. Because the electroweak symmetry is spontaneously broken to $\mathrm{U(1)_{em}}$, three Goldstone bosons are eaten by the $W^\pm$ and Z^0 gauge bosons, and one ends up with two charged Higgs and three neutral Higgs bosons. Due to the Goldstone theorem, the 4×4 (mass)^2 matrix of the neutral Higgs sector is block-diagonalized, i.e., the Goldstone boson ($G^0 = \cos\beta a_1 + \sin\beta a_2$ with $\tan\beta = v_2/v_1$) does not mix with the other neutral bosons, so we have the nontrivial 3×3 (mass)^2 matrix of the three neutral Higgs bosons (following the notation of the third paper of [11–13])

$$\mathcal{M}_{\mathrm{N}}^2 = \begin{pmatrix} \mathcal{M}_{\mathrm{S}}^2 & \widehat{\mathcal{M}}_{\mathrm{SP}}^2 \\ \widehat{\mathcal{M}}_{\mathrm{SP}}^{2\mathrm{T}} & \widehat{\mathcal{M}}_{\mathrm{P}}^2 \end{pmatrix}, \tag{3}$$

where $\mathcal{M}_{\mathrm{S}}^2$, $\widehat{\mathcal{M}}_{\mathrm{SP}}^2$ and $\widehat{\mathcal{M}}_{\mathrm{P}}^2$ are the two-by-two, two-by-one and one-by-one mass matrices of the scalar, scalar–pseudoscalar, and pseudoscalar sectors, respectively. Since there is no mixing between the scalar and pseudoscalar sectors for the vanishing components of $\widehat{\mathcal{M}}_{\mathrm{SP}}^2$, the matrix $\widehat{\mathcal{M}}_{\mathrm{SP}}^2$ contains important parameters, which characterize the Higgs mixing. For a small $\tan\beta$ region, in which the stop contribution is dominant over those of sbottoms and charginos [11–13, 49], the typical sizes of the CP violating off diagonal components are proportional to

$$\frac{1}{16\pi^2}\frac{m_t^4}{v^2}\frac{|\mu|\,|A_t|}{M_{\mathrm{SUSY}}^2}\sin\phi_{CP}^t\,, \tag{4}$$

where m_t are the top quark mass, $\phi_{CP}^t = \arg(A_t\mu) + \xi$ and $v^2 = v_1^2 + v_2^2$. The supersymmetry-breaking scale $M_{\mathrm{SUSY}}^2 = (m_{\tilde{t}_1}^2 + m_{\tilde{t}_2}^2)/2$, where $m_{\tilde{t}_1}$ and $m_{\tilde{t}_2}$ are the lighter and heavier stop masses in (A.18) [50]. The reason why the CPV off diagonal components contain only the terms proportional to the fourth power of m_t in (4) is that the Higgs bilinear soft term m_{12}^2 was eliminated by using the minimum energy condition of the Higgs effective potential with respect to the CP odd field a, i.e., $T_a = \partial\mathcal{V}^{\mathrm{eff}}_{\mathrm{Higgs}}/\partial a = 0$, where $a = -\sin\beta a_1 + \cos\beta a_2$. The various quantitative and qualitative aspects of the dimension-2 parameter m_{12}^2 are discussed in [11–13, 47, 48, 51]. The mass matrix $\mathcal{M}_{\mathrm{N}}^2$ is a real symmetric matrix, and thus can be diagonalized by a 3×3 orthogonal matrix O:

$$O^{\mathrm{T}}\mathcal{M}_{\mathrm{N}}^2 O = \mathrm{diag}\left(M_{H_1}^2, M_{H_2}^2, M_{H_3}^2\right), \tag{5}$$

where $M_{H_1} \le M_{H_2} \le M_{H_3}$. (We follow the notation of the third paper of [11–13], whose order of the Higgs fields is opposite to that in the first paper of [11–13].) The corresponding mass eigenstates H_i ($i = 1, 2, 3$) are defined from the weak eigenstates as

$$(\phi_1, \phi_2, a)^{\mathrm{T}} = O(H_1, H_2, H_3)^{\mathrm{T}}\,. \tag{6}$$

3 Neutral Higgs boson productions at photon colliders

Within both the SM and the MSSM, the neutral Higgs boson decays into two gluons (gg) or two photons ($\gamma\gamma$) have been interesting subjects. The inverse of the former process is the main production mechanism for the neutral Higgs bosons at hadron colliders if the Higgs bosons have intermediate masses. The latter is an important mode for tagging the neutral Higgs bosons at hadron colliders. Its inverse process is the mechanism for neutral Higgs production in $\gamma\gamma$ collisions, which can be run at the international linear collider (ILC).

The reactions $gg \to H_i$ $(i = 1, 2, 3)$ are generated by the (s)quark loops and have already been discussed by two groups in the presence of MSSM Higgs sector CP violation [52–54]. We have calculated these processes and confirmed their results, although they are not reproduced here. The case $\gamma\gamma \to H_i$ is more complicated than the other case $gg \to H_i$, since all the charged particle ($W^\pm$, $H^\pm$ and charginos) contributions must be included as well as the (s)quark loop contributions. In particular, there could be direct CP violation in the decay/production amplitude due to the complex parameters in the chargino mass matrix. This CP violation is independent of the CPV mixing among neutral Higgs bosons and is considered anew in this work. It is straightforward to perform the loop integrations, taking into account the various mixing components for the charginos and neutral Higgs bosons. We present the explicit formulae for the chargino mass matrix $\mathcal{M}_C$, its mass eigenvalues $M_{\tilde{\chi}^-_{1,2}}$, and the two mixing matrices U and V that diagonalize the chargino mass matrix via $U^*\mathcal{M}_C V^{-1} = \mathrm{diag}(M_{\tilde{\chi}^-_1}, M_{\tilde{\chi}^-_2})$ as in Appendix A.

The interaction Lagrangian between the charginos and the three neutral Higgs bosons $H_{j=1,2,3}$ is

$$\mathcal{L}(H_j\tilde{\chi}^+_k\tilde{\chi}^-_l) = H_j\overline{\tilde{\chi}^-_k}\left[\mathrm{Re}\left(\kappa^j_{kl}\right) + \mathrm{i}\gamma^5\,\mathrm{Im}\left(\kappa^j_{kl}\right)\right]\tilde{\chi}^-_l \qquad (7)$$

($j = 1, 2, 3$ and $k, l = 1, 2$), where

$$\kappa^j_{kl} = -\frac{g}{\sqrt{2}}\left[\mathrm{e}^{+\mathrm{i}\xi}U_{k1}V_{l2}(O_{2,j} + \mathrm{i}\cos\beta O_{3,j}) + U_{k2}V_{l1}(O_{1,j} + \mathrm{i}\sin\beta O_{3,j})\right]. \qquad (8)$$

(For completeness, the other relevant couplings are presented in Appendix B.) In this work, it is sufficient to keep only the case of κ^j_{kl} with $k = l$, since we consider the chargino loop contributions to $\gamma\gamma \to H_j$. Note that in the couplings κ^j_{kk} there are three independent CP violating phases $\arg(A_t)$, $\arg(\mu)$ and $\arg(M_2)$ (M_2 is the wino mass) in the basis where the $B\mu$ term is real in the soft SUSY breaking Lagrangian. Also note that the $H_j - \tilde{\chi}^+_k - \tilde{\chi}^-_k$ couplings arise from the Higgs–gaugino–higgsino couplings in the current basis. Thus, the chargino loop effects will be maximized when the wino–higgsino mixing is large. This requires $|\mu| \approx |M_2|$. In our study, however, we are interested in a large μ parameter (which we fix to $|\mu| = 1.2$ TeV) in order to have a large CP mixing between the CP even and CP odd Higgs bosons from the stop loop. For a smaller wino mass parameter $|M_2| = 150$ GeV, the wino–higgsino mixing becomes smaller, but the lighter chargino mass also becomes very light, and the loop function will be enhanced. The net result shows that the light chargino loop effects are important for the reaction $\gamma\gamma \to H_j$, even if the lighter chargino is dominantly a wino state ($|M_2| \ll |\mu|$).

The amplitudes for $\gamma(k_1, \epsilon_1) + \gamma(k_2, \epsilon_2) \to H_i(q)$ $(i = 1, 2, 3)$ should satisfy gauge invariance, and can be defined in terms of two form factors $A_i(s)$ and $B_i(s)$ in a model-independent way as follows (closely keeping the convention of [43, 44]):

$$\mathcal{M}(\gamma\gamma \to H_i) = M_{H_i}\frac{\alpha}{4\pi}\left\{A_i(s)\left[\epsilon_1\cdot\epsilon_2 - \frac{2}{s}(\epsilon_1\cdot k_2)(\epsilon_2\cdot k_1)\right] - B_i(s)\frac{2}{s}\epsilon_{\mu\nu\alpha\beta}\epsilon_1^\mu\epsilon_2^\nu k_1^\alpha k_2^\beta\right\}, \qquad (9)$$

where $s \equiv (k_1 + k_2)^2 = M^2_{H_i}$. Including all the one-loop contributions from charged particles, the CP even form factors A_i at $s = M^2_{H_i}$ are

$$A_i\left(s = M^2_{H_i}\right) = \sum_{f=t,b}A_i^f + \sum_{\tilde{f}_j=\tilde{t}_{1,2},\tilde{b}_{1,2}}A_i^{\tilde{f}_j} + A_i^{H^\pm} + A_i^{W^\pm} + \sum_{j=1,2}A_i^{\tilde{\chi}^\pm_j}, \qquad (10)$$

where the CP even functions A_i^f, $A_i^{\tilde{f}_j}$, $A_i^{H^\pm}$, and $A_i^{W^\pm}$ are given in [43, 44]. We confirmed their results and reproduced them and the related form factor loop functions in Tables 1 and 2 for completeness. Note that the chargino loops contribute to the CP even form factor via

$$A_i^{\tilde{\chi}^\pm_j} = 2\,\mathrm{Re}\left(\kappa^i_{jj}\right)\frac{M_{H_i}}{M_{\tilde{\chi}^-_j}}F_{sf}(\tau_{i\tilde{\chi}^\pm_j}), \qquad (11)$$

Table 1. The amplitudes A_i^X and B_i^X, where i labels three neutral Higgs bosons, and X labels the species of charged particles in the triangle loop with $\tau_{iX} \equiv M^2_{H_i}/4m^2_X$ (see Appendix B and Table 2)

A's and B's	Expressions
A_i^f	$-2(\sqrt{2}G_\mathrm{F})^{1/2}M_{H_i}N_c e_f^2\left(\frac{v_f^i}{R_\beta^f}\right)F_{sf}(\tau_{if})$
$A_i^{\tilde{f}_j}$	$\frac{M_{H_i}N_c e_f^2 g^i_{\tilde{f}_j\tilde{f}_j}}{2m^2_{\tilde{f}_j}}F_0(\tau_{i\tilde{f}})$
$A_i^{W^\pm}$	$(\sqrt{2}G_\mathrm{F})^{1/2}M_{H_i}(c_\beta O_{1,i} + s_\beta O_{2,i})F_1(\tau_{iW})$
$A_i^{H^\pm}$	$\frac{M_{H_i}vC_i}{2m^2_{H^\pm}}F_0(\tau_{iH})$
$A_i^{\tilde{\chi}^\pm_j}$	$2\,\mathrm{Re}\left(\kappa^i_{jj}\right)\frac{M_{H_i}}{M_{\tilde{\chi}^-_j}}F_{sf}(\tau_{i\tilde{\chi}^\pm_j})$
B_i^f	$2(\sqrt{2}G_\mathrm{F})^{1/2}M_{H_i}N_c e_f^2\left(\frac{\overline{R}^f_\beta a^i_f}{R^f_\beta}\right)F_{pf}(\tau_{if})$
$B_i^{\tilde{\chi}^\pm_j}$	$-2\,\mathrm{Im}\left(\kappa^i_{jj}\right)\frac{M_{H_i}}{M_{\tilde{\chi}^-_j}}F_{pf}(\tau_{i\tilde{\chi}^\pm_j})$

Table 2. Form factor loop functions F in terms of the scaling function $f(\tau)$ defined in (12)

F	Definitions
$F_{sf}(\tau)$	$\tau^{-1}[1+(1-\tau^{-1})f(\tau)]$
$F_{pf}(\tau)$	$\tau^{-1}f(\tau)$
$F_0(\tau)$	$\tau^{-1}[-1+\tau^{-1}f(\tau)]$
$F_1(\tau)$	$2+3\tau^{-1}+3\tau^{-1}(2-\tau^{-1})f(\tau)$

where $\tau_{iX}=M_{H_i}^2/4M_X^2$. The form factor loop function $F_{sf}(\tau)=\tau^{-1}[1+(1-\tau^{-1})f(\tau)]$ (and other loop functions defined in Table 2) depends on the scaling function $f(\tau)$ [1]:

$$f(\tau)=-\frac{1}{2}\int_0^1\frac{\mathrm{d}y}{y}\log[1-4\tau y(1-y)] =\begin{cases}\arcsin^2(\sqrt{\tau}) & \text{for } \tau\le 1\,,\\ -\frac{1}{4}\left[\log\left(\frac{\sqrt{\tau}+\sqrt{\tau-1}}{\sqrt{\tau}-\sqrt{\tau-1}}\right)-\mathrm{i}\pi\right]^2 & \text{for } \tau\ge 1\,.\end{cases} \tag{12}$$

On the other hand, the CP odd form factors B_i receive contributions only from the fermion loops and not from the boson loops:

$$B_i\big(s=M_{H_i}^2\big)=\sum_{f=t,b}B_i^f+\sum_{j=1,2}B_i^{\tilde{\chi}_j^\pm}\,, \tag{13}$$

where the SM fermion loop contributions (the B_i^f) are found in [43, 44] (see Tables 1 and 2). The chargino contributions are represented as

$$B_i^{\tilde{\chi}_j^\pm}=-2\,\mathrm{Im}\left(\kappa_{jj}^i\right)\frac{M_{H_i}}{M_{\tilde{\chi}_j^-}}F_{pf}(\tau_{i\tilde{\chi}_j^\pm})\,, \tag{14}$$

where $F_{pf}(\tau)=\tau^{-1}f(\tau)$. Thus, in the CP conserving limit, only the SM fermion loops (and not boson loops) contribute to the production reaction $\gamma\gamma\to A$ of the CP odd neutral Higgs boson A at photon colliders. Therefore, the CP violating effect from the chargino loops would be prominent in the process $\gamma\gamma\to H_2$.

It is also convenient to use the two helicity amplitudes $\mathcal{M}_{++}^{(j)}$ and $\mathcal{M}_{--}^{(j)}$ $(j=1,2,3)$ from

$$\mathcal{M}_{\lambda_1\lambda_2}^{(j)}=-M_{H_j}\frac{\alpha}{4\pi}\{A_j(s)\delta_{\lambda_1\lambda_2}+\mathrm{i}\lambda_1 B_j(s)\delta_{\lambda_1\lambda_2}\}\,, \tag{15}$$

where $\lambda_{1,2}=\pm$ denote the photon helicities. Then, in the narrow-width approximation, the partonic cross sections of the s-channel Higgs production [43, 44] are

$$\sigma(\gamma\gamma\to H_i)=\frac{\pi}{4M_{H_i}^4}\left(|\mathcal{M}_{++}^{(i)}|^2+|\mathcal{M}_{--}^{(i)}|^2\right)\delta\big(1-M_{H_i}^2/s\big) \equiv\hat{\sigma}_0(H_i)\delta\big(1-M_{H_i}^2/s\big)\,. \tag{16}$$

By using the amplitudes of $\gamma\gamma\to H_i$ $(i=1,2,3)$ at $s=M_{H_i}^2$, we can also obtain the unpolarized decay rates of the neutral Higgs bosons into two photons,

$$\Gamma(H_i\to\gamma\gamma)=\frac{\alpha^2}{256\pi^3}M_{H_i} \times\left(\left|A_i\big(s=M_{H_i}^2\big)\right|^2+\left|B_i\big(s=M_{H_i}^2\big)\right|^2\right)\,. \tag{17}$$

The Higgs sector CP violation can be measured in the following three polarization asymmetries $\mathcal{A}_a$ $(a=1,2,3)$ [27, 28] defined in terms of two independent helicity amplitudes $A_i(s)$ and $B_i(s)$:

$$\mathcal{A}_1(H_i)=\frac{|\mathcal{M}_{++}^{(i)}|^2-|\mathcal{M}_{--}^{(i)}|^2}{|\mathcal{M}_{++}^{(i)}|^2+|\mathcal{M}_{--}^{(i)}|^2}=\frac{2\,\mathrm{Im}[A_i(s)B_i(s)^*]}{|A_i(s)|^2+|B_i(s)|^2}\,, \tag{18}$$

$$\mathcal{A}_2(H_i)=\frac{2\,\mathrm{Im}(\mathcal{M}_{--}^{(i)*}\mathcal{M}_{++}^{(i)})}{|\mathcal{M}_{++}^{(i)}|^2+|\mathcal{M}_{--}^{(i)}|^2}=\frac{2\,\mathrm{Re}[A_i(s)B_i(s)^*]}{|A_i(s)|^2+|B_i(s)|^2}\,, \tag{19}$$

$$\mathcal{A}_3(H_i)=\frac{2\,\mathrm{Re}(\mathcal{M}_{--}^{(i)*}\mathcal{M}_{++}^{(i)})}{|\mathcal{M}_{++}^{(i)}|^2+|\mathcal{M}_{--}^{(i)}|^2}=\frac{|A_i(s)|^2-|B_i(s)|^2}{|A_i(s)|^2+|B_i(s)|^2}\,. \tag{20}$$

In the CP conserving limit, one of the form factors A_i and B_i must vanish, and thus $\mathcal{A}_1=\mathcal{A}_2=0$, and $\mathcal{A}_3=+1$ (-1) for a pure CP even (CP odd) Higgs scalar. From the definition of the function $f(\tau)$ in (12), we find that the form factors A_i and B_i may be complex when the Higgs masses M_{H_i} are two times larger than the particle mass in the loop. This will induce rich structures in the polarization asymmetries $\mathcal{A}_a$ as functions of Higgs masses and other SUSY parameters in the presence of Higgs sector CP violation.

Finally, the number of events can be estimated by the combination of the luminosity and the cross section for $\gamma\gamma\to H_{i=1,2,3}$. Although the photon beam luminosity depends on many parameters, if one considers only the high energy part of the generated photons, the conversion factor (~ 0.3) and the photon spot size comparable to that of electron beam, the approximate luminosity of the $\gamma\gamma$ collider [56, 57] is

$$\mathcal{L}^{\gamma\gamma}\approx 0.3^2\mathcal{L}_{\mathrm{geom}}^{ee}\approx 0.1\mathcal{L}_{\mathrm{geom}}^{ee}\,, \tag{21}$$

where $\mathcal{L}_{\mathrm{geom}}^{ee}$ is the luminosity of the e^+e^- collider. Taking $100\,\mathrm{fb}^{-1}$ as a nominal integrated luminosity in the $\gamma\gamma$ mode, we can expect 100 events per year if the production cross section is 1 fb.

4 Numerical analyses

There are three independent complex phases, $\arg(M_2)$, $\arg(\mu)$ and $\arg(A_t)$, that could be relevant to CP violating Higgs mixing (called indirect CP violation) and direct CP violation in the production or the decay $\gamma\gamma\leftrightarrow H_i$. The CP violation in the neutral Higgs sector through the stop loop contributions with the complex A_t parameter always

Table 3. CP violations from three independent phases for moderate $\tan\beta \lesssim 20$

Phase	Indirect mixing	Direct CPV
$\arg(A_t)$	Yes	Yes
$\arg(M_2)$	Small	Yes
$\arg(\mu)$	Yes	Yes

appears in the combination of $\arg(A_t\mu)$. For the complex M_2 parameter, the chargino mass matrix will contain CP violation, and thereby there would be additional CP violating effects in the chargino loop contributions to $\gamma\gamma \to H_i$. However, this CP violating effect is independent of CP violation of the neutral Higgs sector resulting in the mixing between the CP even and the CP odd Higgs bosons for $\tan\beta \lesssim 20$ [49]. Note that values of $\tan\beta \lesssim O(3)$ in the CP violating MSSM are not favored by the data collected by the four LEP collaborations [46]. In Table 3, we list the effects of the CPV phases on both indirect and direct CP violation.

In general, all the three phases can be nonzero simultaneously, generating CP violations in the mixing as well as in the decay (or production). In order to see the effect of each phase, let us consider the following simplified cases separately.

- Case I: the chargino loop in the CP conserving limit.
- Case II: nonvanishing $\arg(A_t)$. In this case, there are CP violations both in the mixing and in the production/decay from stop loops. The chargino loop contributions are CP conserving in this case.
- Case III: nonvanishing $\arg(M_2)$. In this case, the CP violating Higgs mixing due to the chargino loops is small for $\tan\beta \lesssim 20$, and only the direct CP violation is important.
- Case IV: nonvanishing $\arg(\mu)$. In this case, there are CP violations both in the mixing and in the production/decay.
- Case V: fixed μ and M_2 phases from $e^+e^- \to \chi_i^+\chi_j^-$, and the unknown A_t phase. We set $\arg(\mu) = \arg(M_2) = 45°$, and vary $\arg(A_t)$.

For numerical analyses, we fix the parameters as follows. First, $A_t = A_b$ is assumed for simplicity, even if these couplings are independent in general. Secondly, in order to investigate the chargino contributions more clearly (see the discussion following (8)) the chosen parameter set is composed of

$$|A_t| = |A_b| = \frac{|\mu|}{3} = 0.4\,\text{TeV}\,, \quad |M_2| = 0.15\,\text{TeV}\,,$$
$$\tan\beta = 10\,, \quad M_{\text{SUSY}} = 0.5\,\text{TeV}\,. \tag{22}$$

Using this set of parameters, we will study in detail $\hat{\sigma}_0(\gamma\gamma \to H_i)$ and $\mathcal{A}_a(H_i)$ as functions of each Higgs boson mass M_{H_i} and the CP violating phases with/without the chargino loop contributions. Because the A_t phase is strongly constrained by the two-loop Barr–Zee type contributions to the EDMs of electron and neutron, we do not consider the case of very large $\tan\beta$.

4.1 Case I: chargino loop contributions in the CP conserving limit

It turns out that the Higgs sector CP violation is most prominent in the would-be CP odd Higgs boson H_2 production at photon colliders. Therefore, the production of the would-be CP odd Higgs scalar is first discussed. In Fig. 1, we show the production cross sections for $\gamma\gamma \to H_2$ and $\gamma\gamma \to H_3$ as the functions of real M_2 in the CP conserving limit (i.e., $\arg(A_t) = \arg(M_2) = \arg(\mu) = 0°$). In both cases, we assumed a real $\mu = 1.2$ TeV, and set $M_{H^+} = 300$ GeV, so that $M_{H_2} = 290$ GeV for $\tan\beta = 10$. The solid (dash-dotted) curve represents the case with (without) the chargino contributions. For vanishing A_t and μ phases, H_2 will be the pure CP odd state (A) for our parameter set (22). In this case, $\hat{\sigma}_0(\gamma\gamma \to H_2)$ can receive contributions only from the fermion loops, since the couplings of H_2 to the sfermion, charged Higgs boson and W-boson pairs vanish in the CP conserving limit. The cross section for $\gamma\gamma \to H_2$ without the chargino loop contributions is independent of M_2 (thus there appear the horizontal dash-dotted lines), and is quite small ($\lesssim 0.1$ fb). The bot-

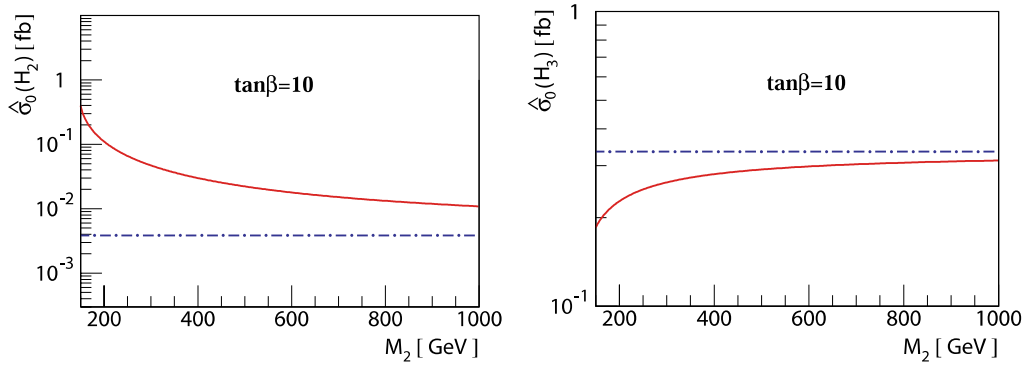

Fig. 1. In Case I, the cross sections for $\gamma\gamma \to H_2$ (*left*) and $\gamma\gamma \to H_3$ (*right*) with the chargino loop contributions (*solid curve*) and without the chargino loop contributions (*dash-dotted horizontal line*) in units of fb as functions of M_2 with $\tan\beta = 10$. We choose $M_{H^+} = 300$ GeV and $\arg(A_t) = \arg(\mu) = \arg(M_2) = 0°$ for the parameter set (22)

tom quark contribution is negligible compared to the top quark contribution for two reasons: (i) the small b quark mass, and (ii) the smaller electric charge of b quark due to the production amplitude $\propto e_{\rm q}^2$. For our choice of parameters, it turns out that the bottom quark contribution can be safely neglected for $\tan\beta \lesssim 10$. On the other hand, the cross section for $\gamma\gamma \to H_2$ is enhanced almost by an order of magnitude, when the chargino loop contributions are included. The chargino loop contributions to $\gamma\gamma \to H_2$ cannot be ignored at all, if charginos are not very heavy. This is true even in the case of $|M_2| \ll |\mu|$, where the wino–higgsino mixing is not large. The lighter chargino is still light enough ($|M_2| = 150\,\text{GeV}$ for our parameter set) and the loop contribution is important. In addition, due to the $\frac{1}{\tan\beta}$ suppression factor for the top loop, the chargino loop contributions become more important for larger $\tan\beta$. Finally, as M_2 increases, the lighter chargino becomes heavier, and then the chargino loop contributions decrease rather quickly due to the decoupling theorem. Since the chargino masses arise dominantly from the SUSY breaking rather than from the electroweak symmetry breaking, the decoupling mechanism is more effective for the chargino loop contributions than the top loop one.

4.2 Case II: nonvanishing $\arg(A_t)$

In the case that $\arg(A_t)$ is the only CP violating phase, there are CP violations both in the Higgs mixing and in the production/decay from stop loops, but the chargino loop contributions are CP conserving. We want to analyze this case in order to compare our results with the previous ones of [64], where the chargino loop contributions were neglected by the decoupling mechanism of very heavy charginos. On the other hand, purely direct CP violating effects from the chargino loops will be discussed in the following subsection for Case III.

In Fig. 2, we show the cross section for $\gamma\gamma \to H_2$ as a function of $\arg(A_t)$ for $\tan\beta = 10$. The solid (dotted) curves represents the case with (without) the chargino loop contributions. For $\arg(A_t) = 0^\circ$ (or 180°), the cross section is strongly enhanced by the chargino loop contributions as discussed in the previous subsection. As $\arg(A_t)$ is turned on, the cross section is significantly enhanced even without the chargino loop contributions. The reason for this enhancement can be that all the charged particles including bosons begin to contribute in the presence of CP violation in the Higgs sector. The dotted curve strongly depends on $\arg(A_t)$ for the following reasons.

First of all, the mixing angles sensitively depend on $\arg(A_t)$. Since the mixing between the CP even and CP odd neutral Higgs bosons arises from the stop loops (see (4)), the A_t phase affects the CP mixing through $\mathrm{Im}(A_t\mu)$ in (4). In addition, once CP is broken in the Higgs sector, all the charged particles including bosons as well as fermions contribute to $\gamma\gamma \to H_2$. Thus, the scalar particles of stops can contribute to the H_2 production showing the dependence on $\arg(A_t)$. The stop masses in the triangle loop of $\gamma\gamma \to H_2$ can give a strong phase dependence to the Higgs production cross section, since the

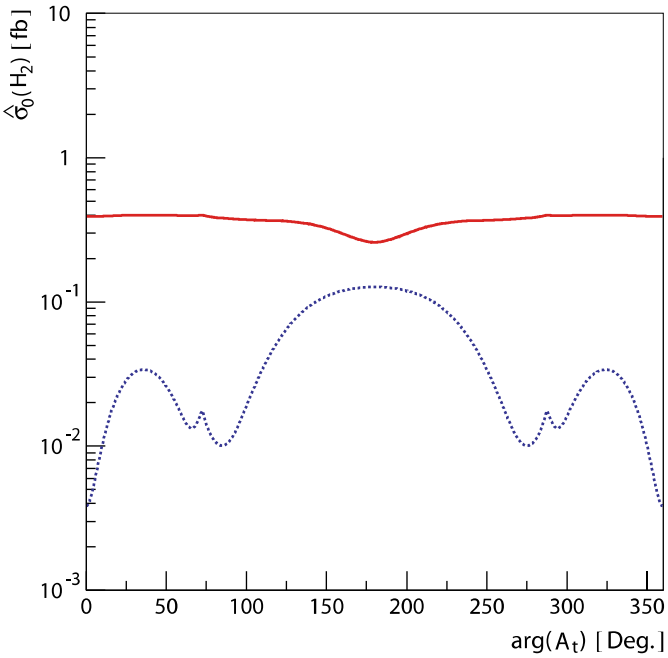

Fig. 2. In Case II, the cross sections for $\gamma\gamma \to H_2$ with the chargino loop contributions (*solid curve*) and without the chargino loop contributions (*dotted curve*) in units of fb as a function of $\arg(A_t)$ for $M_2 = 150\,\text{GeV}$. The phases of μ and M_2 are set to zero

LR mixing term $m^2_{\tilde{t}\rm LR} = m_t(A_t^* \mathrm{e}^{-\mathrm{i}\xi} - \mu/\tan\beta)$ in (A.15) of Appendix A depends sensitively on the A_t phase especially for $|A_t| \sim |\mu/\tan\beta|$. In the meantime, the dominant contribution still comes from the chargino loops (see the solid curves in Fig. 2). The net result depends on $\arg(A_t)$ rather mildly, mainly through the A_t phase of the CP odd and CP even Higgs mixing. In addition, note that the sensitivity of the cross section $\hat{\sigma}_0(\gamma\gamma \to H_2)$ to $\arg(A_t)$ may increase as $\tan\beta$ decreases. This tendency can be understood by the phase dependencies of the stop masses, since stop loops contribute to the triangle-loop diagrams. The stop mass eigenvalues are maximally sensitive to the CP phase $\arg(A_t)$ when $|A_t| = |\mu|/\tan\beta$ due to the LR mixing (i.e., $\tan\beta|_{\rm m.s.} = 3$ for our parameter set $|A_t| = |\mu|/3$), so the stop masses are less sensitive to the CP phase $\arg(A_t)$ for the larger $\tan\beta = 10$. Therefore, the phase dependence of the cross section is a decreasing function of $\tan\beta$ for $\tan\beta \gtrsim O(3)$ in our choice of SUSY parameter set.

In Fig. 3, the cross sections $\hat{\sigma}_0(H_i)$ $(i = 1, 2, 3)$ in units of fb are presented for five different A_t phases: $\arg(A_t) = 0^\circ$ (thick solid curve), 40° (dash-dotted curve), 80° (dashed curve), 120° (dotted curve) and 160° (solid curve) for $\tan\beta = 10$. Since it was shown from Fig. 2 that the chargino loop contributions are important for the production cross sections, they are included in Fig. 3 with $M_2 = 150\,\text{GeV}$ for which $M_{\tilde{\chi}_1^-} = 148.2\,\text{GeV}$. The chargino contributions to $\gamma\gamma \to H_1$ are negligible, since M_{H_1} is far below the chargino pair threshold $2M_{\tilde{\chi}_1^-}$ for our parameter set. On the other hand, two heavier Higgs productions are affected by the chargino loops by significant amounts,

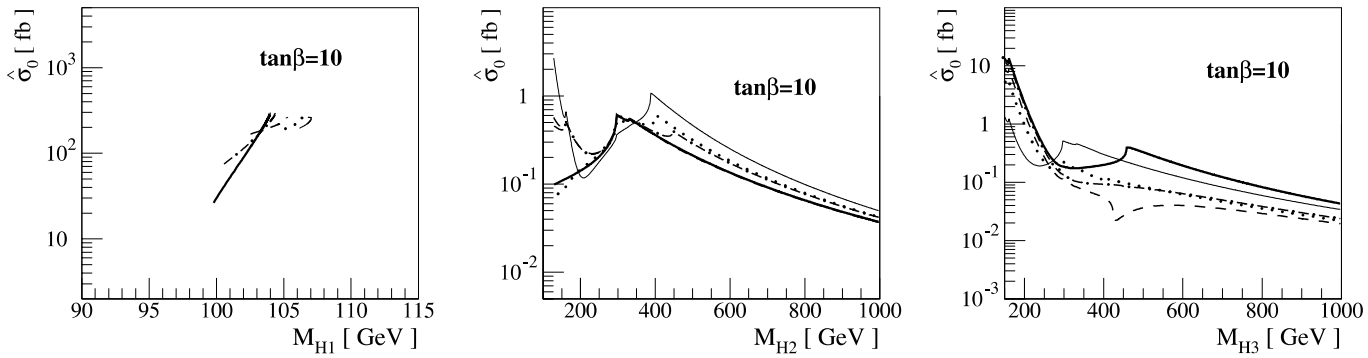

Fig. 3. In Case II, the unpolarized cross sections for $\gamma\gamma \to H_i$ $(i = 1, 2, 3)$ with the chargino loop contributions for $\tan\beta = 10$ and $M_2 = 150$ GeV in units of fb as functions of each Higgs mass for five different values of the A_t phase: $\arg(A_t) = 0^\circ$ (*thick solid curve*), 40° (*dash-dotted curve*), 80° (*dashed curve*), 120° (*dotted curve*) and 160° (*solid curve*). The phases of μ and M_2 are set to zero

and we can observe rich structures in the production cross sections due to the interference among the contributions of all the charged particles. For example, if the chargino loop contributions are not included, the production cross section for $\gamma\gamma \to H_2$ will have only a single peak at the point $M_{H_2} = 2m_t$ for $\arg(A_t) = 0^\circ$. However, due to the chargino contributions, the production cross section shows two comparable peaks at the points $M_{H_2} = 2M_{\tilde{\chi}_1^-}$ (lighter chargino) and $M_{H_2} = 2m_t$ in the CP conserving limit. As the CP violating phase $\arg(A_t)$ increases, the cross section $\hat{\sigma}_0(\gamma\gamma \to H_2)$ starts to get extra contributions from the charged boson loops (involving the sfermions, charged Higgs boson and the W-boson pairs) due to the mixing between the CP odd and CP even neutral Higgs bosons.

We can consider some $\tan\beta$ dependencies in terms of three aspects: (i) the effect of bottom quark loop contribution, (ii) the dominant chargino loop contributions, and (iii) the interchange of the CP properties of the neutral Higgs bosons.

- Since the bottom quark Yukawa coupling (to the CP even Higgs boson) is proportional to $1/\cos\beta$, the bottom quark contribution can be significant in the region of large $\tan\beta$. For $\arg(A_t) = 0^\circ$, the CP odd Higgs boson H_2 has pseudoscalar couplings to the top and bottom quarks, where the coupling of H_2 to the top (bottom) quark is proportional to $\cot\beta$ ($\tan\beta$) (see (B.1) and (B.2) of Appendix B). Furthermore, there are additional differences from different electric charges of the top and bottom quarks, since the $\gamma\gamma \to H_i$ amplitudes depend on e_q^2, which are $(2/3)^2$ versus $(-1/3)^2$ for the (s)top and (s)bottom, respectively. On the other hand, the loop functions have weaker $\tan\beta$ dependencies. For our parameter set, it turns out that the bottom quark contribution begins to dominate the top quark contribution for $\tan\beta \sim 10$.
- In the CP conserving limit, the chargino contributions to $\gamma\gamma \to A$ are dominant over the top quark contribution, since the latter is suppressed by $\frac{1}{\tan\beta}$ relative to the former in spite of assuming the $O(0.1)$ mixing angles in the chargino sector. This may imply that the top quark contribution decreases more quickly than the lighter chargino contribution (i.e., there occurs a higher peak at the chargino pair threshold) as $\tan\beta$ increases.
- The final point is the interchange of the CP properties of the heavier Higgs bosons H_2 and H_3 for large $\arg(A_t)$ and large $\tan\beta = 10$. Since there are only fermion contributions to the CP odd Higgs production, i.e., two peaks at $M_{H_i} = 2M_{\tilde{\chi}_1^-}$ and $2m_t$, we can find from Fig. 3 that H_3 for $\arg(A_t) = 160^\circ$ has the same CP odd property as H_2 for $\arg(A_t) = 0^\circ$. This can be checked even more easily by using the polarization asymmetry $\mathcal{A}_3$, which is $+1$ (-1) for a CP even (CP odd) Higgs boson, as discussed below in relation with the polarization asymmetries (Figs. 4 and 5).

In the meantime, since the importance of the chargino loop contributions for H_3 production is also similar to the case of H_2 production as discussed above, we will not repeat it.

Assuming $100\,\mathrm{fb}^{-1}$ as a nominal integrated luminosity in the $\gamma\gamma$ mode, we can infer from Fig. 3 that the maximum number of events for the CP odd Higgs boson is approximately 1 per a year for $\tan\beta = 10$, when the unpolarized cross section does not contain the chargino loop contributions. However, the chargino loop contributions enhance the maximum number of events as approximately 71. Hence, the chargino loop contributions for the production of the would-be CP odd Higgs boson can be significant at the $\gamma\gamma$ collider.

In Fig. 4, three polarization asymmetries of H_2 are shown as functions of $\arg(A_t)$. We choose $M_{H^+} = 300$ GeV as in Fig. 1 so that $M_{H_2} = 290$ GeV. The case with (without) chargino loops is represented by solid (dash-dotted) curves. The polarization asymmetries $\mathcal{A}_a(\Phi)$ satisfy the following relations:

$$\mathcal{A}_{1,2}(\Phi) = -\mathcal{A}_{1,2}(360^\circ - \Phi)\,, \quad \mathcal{A}_3(\Phi) = +\mathcal{A}_3(360^\circ - \Phi)\,, \tag{23}$$

where $\Phi = \arg(A_t\mu) + \xi$ with $\xi \simeq 0$. Namely, $\mathcal{A}_{1,2}$ are CP odd observables (antisymmetric about $\Phi = 180^\circ$), and $\mathcal{A}_3$ is a CP even observable (symmetric about $\Phi = 180^\circ$). It is noteworthy that the chargino loops not only enhance the cross sections but also affect the polarization asymmetries by significant amounts.

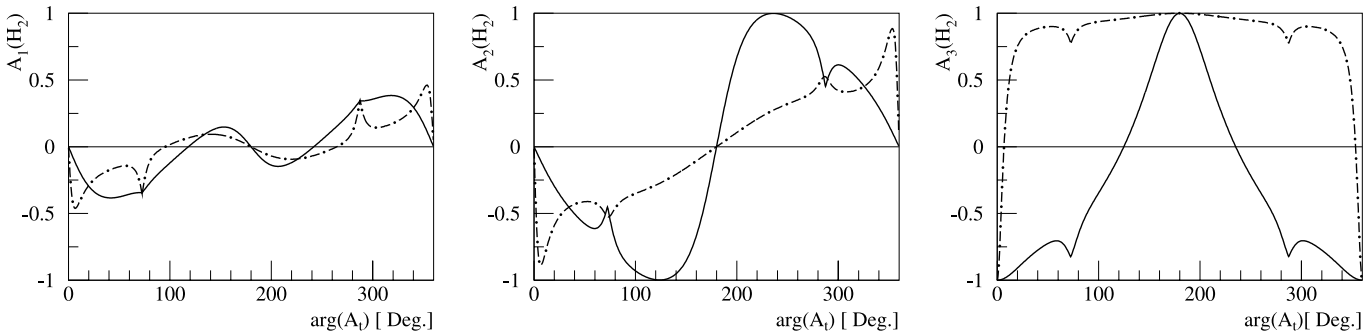

Fig. 4. In Case II, the polarization asymmetries $\mathcal{A}_a$ $(a = 1, 2, 3)$ without (*dash-dotted curve*) and with (*solid curve*) the chargino loop contributions as functions of $\arg(A_t)$. We take $M_{H^+} = 300$ GeV and $\arg(\mu) = \arg(M_2) = 0^\circ$ for the parameter set (22)

In Fig. 5, we present the polarization asymmetries $\mathcal{A}_a(H_i)$ $(a, i = 1, 2, 3)$ as functions of the neutral Higgs masses for $\arg(A_t) = 0^\circ$, 40°, 80°, 120° and 160°, including all the charged particles in the loops. The lightest Higgs boson H_1 behaves like a CP even scalar for $\tan\beta = 10$, since $-0.1\% \lesssim \mathcal{A}_1 \leq 0$, $0 \leq \mathcal{A}_2 \lesssim 0.3\%$, and $\mathcal{A}_3 \simeq 1$. If $\tan\beta$ becomes larger, the top (stop) loop contribution is accompanied by the bottom (sbottom) contribution to the polarization asymmetries of the heavier Higgs bosons H_2 and H_3. According to Fig. 5, it should be indicated that as the CP violating phase $\arg(A_t)$ increases for the case of large $\tan\beta$, the value of the asymmetry $\mathcal{A}_3$ of H_2 approaches that of H_3 at $\arg(A_t) = 0^\circ$ and vice versa, i.e., the CP properties of the heavier Higgs bosons H_2 and H_3 can be interchanged.

From Fig. 5, the polarization asymmetry $\mathcal{A}_2(H_1)$ is the most sensitive CP observable in detecting the CP violation of the lightest Higgs boson for rather large $\tan\beta$, when the chargino contribution is included. This result is different from [43], where charginos are neglected by assuming that they are very heavy. Unfortunately, the asymmetry itself is too small, so that it would not be easy to detect nonzero $\mathcal{A}_2(H_1)$. However, the asymmetries for the heavier neutral Higgs bosons H_2 and H_3 can be sizable enough to be used as probes of Higgs sector CP violation, if they are produced with high statistics at NLCs. Therefore, it is necessary to prepare the colliding photon beams with large linear polarizations as well as a high center of mass energy $\sqrt{s_{\gamma\gamma}}$ in order to produce the neutral Higgs bosons and determine their CP properties in a model independent manner.

4.3 Case III: purely direct CP violation from nonvanishing $\arg(M_2)$

Until now, we have analyzed the cross sections and asymmetries of the neutral Higgs mass eigenstates by varying $\arg(A_t)$ alone. Since there are other possible CP violating phases such as $\arg(\mu)$ and $\arg(M_2)$, further analyses with those phases are to be performed. From the previous figures, we can easily expect that for the parameter set (22) the contribution of charginos is dominant over those of the others by comparing the cross sections and asymmetries with the chargino contribution to those without it. Therefore, we will always include the chargino loop contributions and no longer discuss the situations without the chargino loops from now on.

In Case III with $\arg(A_t) = 0^\circ$, there is no considerable CP violating mixing between the neutral Higgs bosons for $\tan\beta \lesssim 20$. However, the phase in M_2 can generate direct CP violations in $\gamma\gamma \to H_i$ through the chargino loop diagrams.

- The H_j–$\tilde{\chi}_k^+$–$\tilde{\chi}_l^-$ couplings have strong phase dependencies on both $\arg(\mu)$ and $\arg(M_2)$, since the off diagonal components of the chargino mixing matrices U and V are sensitive to those phases.
- Meanwhile, from numerical work, we were able to ascertain that the coupling constants κ_{kk}^j of the H_j–$\tilde{\chi}_k^+$–$\tilde{\chi}_l^-$ vertices in (8) are insensitive to the A_t phase for our parameter set – this was expected from Fig. 2 to some extent.
- Due to $|M_2| \ll |\mu|$ for our parameter set, we can find from (A.11) that the masses of the charginos are nearly independent of the μ and M_2 phases. This implies that the loop function part is almost the same for any variations of the CP violating phases.

Since the mass of the lightest Higgs H_1 is smaller than that of the lighter chargino for our parameter set (22), its production amplitude receives little contribution from the charginos, and thus we will consider only the heavier Higgs bosons, H_2 and H_3. In Fig. 6, we show the cross sections for H_2 and H_3 production with nonvanishing M_2 phase. It can easily be noted that the cross sections are symmetric about the CPV phase $= 180^\circ$ due to the CP natures of the A and B form factors, and that they have stronger dependencies on the M_2 phase than on the A_t phase for our parameter set. It is observed that the cross section of H_3 production has a weaker dependence on the M_2 phase than that of H_2 production for the parameter set.

In Fig. 7, the cross sections for $\gamma\gamma \to H_{i=1,2,3}$ are shown as functions of the neutral Higgs boson masses M_{H_i} for different values of $\arg(M_2)$. Again we observe the threshold behaviors when M_{H_i} is equal to twice the value of the masses of the charged particles in the loop. For the heavier neutral Higgs bosons, the production cross section is smaller than 1 fb in most of the parameter space, and it would be difficult to produce and study them directly at photon colliders.

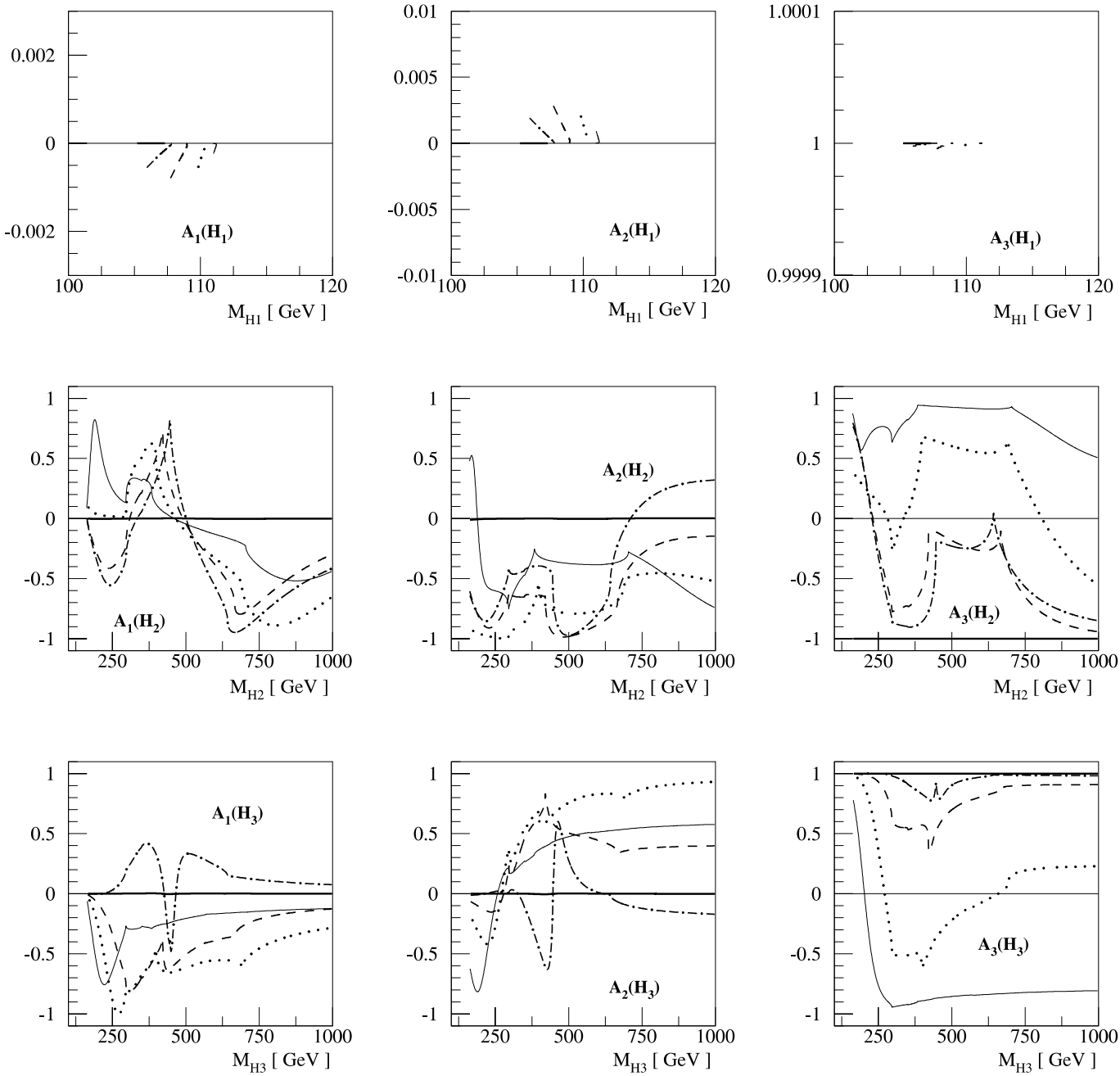

Fig. 5. In Case II, the polarization asymmetries $\mathcal{A}_a$ $(a = 1, 2, 3)$ with the chargino loop contributions as functions of each Higgs mass for five different values of the A_t phase: $\arg(A_t) = 0^\circ$ (*thick solid curve*), 40° (*dash-dotted curve*), 80° (*dashed curve*), 120° (*dotted curve*) and 160° (*solid curve*). We choose $\arg(\mu) = \arg(M_2) = 0^\circ$ for the parameter set (22)

In Fig. 8, including the chargino contributions, we present the polarization asymmetries $\mathcal{A}_a$ $(a = 1, 2, 3)$ of H_2 and H_3 as functions of $\arg(M_2)$. In this case, any nonzero values of polarization asymmetries $\mathcal{A}_a$ can be taken as clear indications of direct CP violations in the $\gamma\gamma \to H_i$, since the CP violation in the mixing from $\arg(M_2)$ is negligible for $\tan\beta \lesssim 20$. From the analysis of the chargino mixing angles in Appendix A, it can easily be checked that for $\arg(A_t) = \arg(\mu) = 0^\circ$, the asymmetries $\mathcal{A}_{1,2}(H_2)$ and $\mathcal{A}_3(H_2)$ are antisymmetric (i.e., CP odd observables) and symmetric (i.e., a CP even observable) about $\arg(M_2) = 180^\circ$. A similar argument is applied to the figures for varying the μ phase. Thus, in both cases, the asymmetries have strong sensitivities to the CP violating phases. However, because for $\tan\beta \lesssim 20$ the M_2 phase participates only in the triangle diagram of the $\gamma\gamma \to H_i$ (i.e., H_2 is nearly the pure CP odd state A), there occur differences between Figs. 8 and 11, treated in the next subsection. On the other hand, it seems that the asymmetries of H_3 are less sensitive to the M_2 and μ phases than those of H_2.

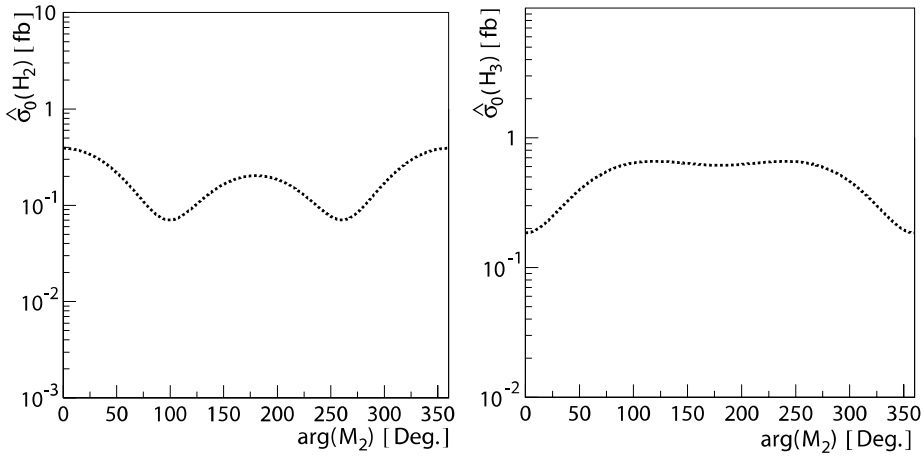

Fig. 6. In Case III, the cross sections for $\gamma\gamma \to H_2$ (*left*) and $\gamma\gamma \to H_3$ (*right*) in units of fb as functions of $\arg(M_2)$. We choose $M_{H^+} = 300\,\text{GeV}$ and $\arg(A_t) = \arg(\mu) = 0^\circ$ for the parameter set (22)

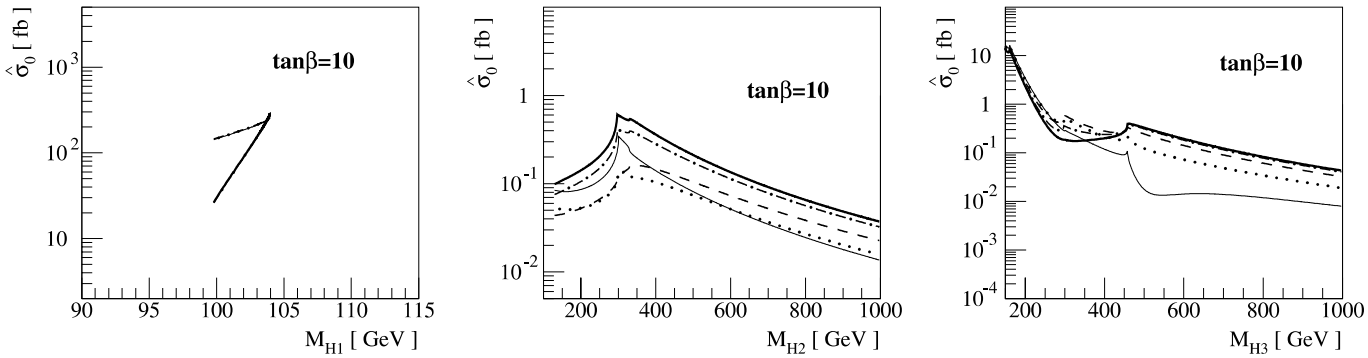

Fig. 7. In Case III, the unpolarized cross sections for $\gamma\gamma \to H_i$ $(i = 1, 2, 3)$ for $M_2 = 150\,\text{GeV}$ in units of fb as functions of each Higgs mass for five different values of the M_2 phase: $\arg(M_2) = 0^\circ$ (*thick solid curve*), 40° (*dash-dotted curve*), 80° (*dashed curve*), 120° (*dotted curve*) and 160° (*solid curve*). The phases of μ and A_t are set to zero

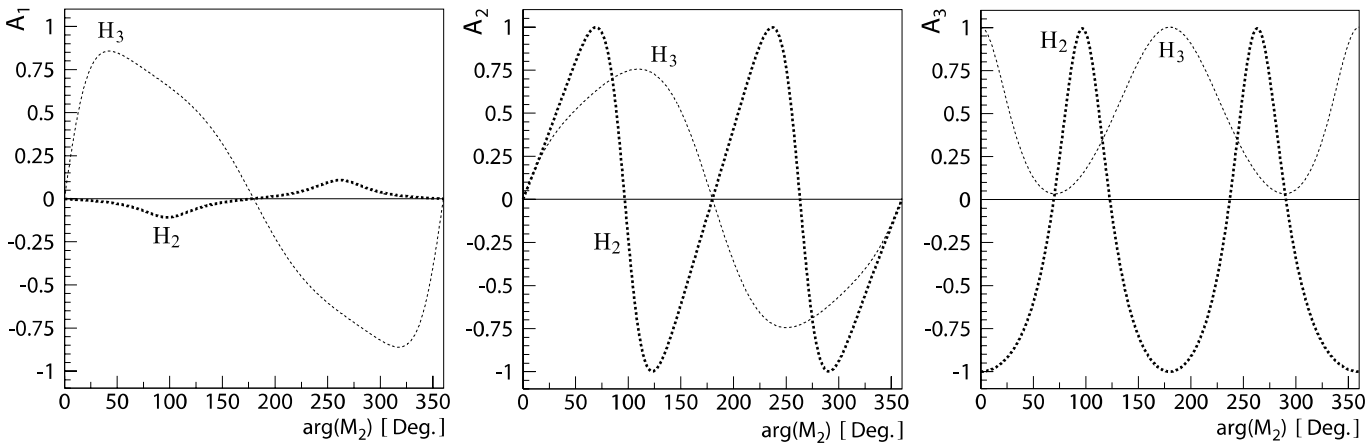

Fig. 8. In Case III, the polarization asymmetries $\mathcal{A}_a$ $(a = 1, 2, 3)$ of H_2 (*thick dotted curve*) and H_3 (*dotted curve*) with the chargino loop contributions as functions of $\arg(M_2)$. We choose $M_{H^+} = 300\,\text{GeV}$ and $\arg(A_t) = \arg(\mu) = 0^\circ$ for the parameter set (22)

4.4 Case IV: nonvanishing $\arg(\mu)$

Because the μ phase is the only source of CP violation, there occur direct CP violations in $\gamma\gamma \to H_i$ from the chargino loop contributions as in Case III of the CP violating M_2 phase. In addition, there must exist indirect CP violating mixing in the neutral Higgs bosons from the stop loop contributions in (4). Therefore, the structures in the CP violating observables will be richer than those in Case II of the nonvanishing A_t phase. The observations made in Case III are still valid for nonzero μ phase, and we do not repeat them here.

In Fig. 9, we show the production cross sections for H_2 and H_3 at photon colliders as functions of the μ phase. It can easily be noted that the cross sections are symmetric about the $\arg(\mu) = 180^\circ$ due to the CP natures of the A and B form factors. The cross sections depend more strongly on the μ phase than on the A_t phase for our parameter set. In Fig. 10, the cross sections for $\gamma\gamma \to H_{i=1,2,3}$ are presented as functions of M_{H_i} for $\tan\beta = 10$. The cross section for H_1 is quite large and depends strongly on the μ phase. On the other hand, the cross sections for H_2 and H_3 are smaller than 1 fb in most of the parameter space, and it would not be easy to produce them at photon colliders.

In Fig. 11, we present the polarization asymmetries $\mathcal{A}_a$ $(a = 1, 2, 3)$ of H_2 and H_3 as functions of $\arg(\mu)$. From the analysis of the chargino mixing angles in Appendix A, it can easily be checked that for $\arg(A_t) = \arg(M_2) = 0^\circ$, the asymmetries $\mathcal{A}_{1,2}(H_j)$ and $\mathcal{A}_3(H_j)$ are antisymmetric (i.e., CP odd observables) and symmetric (i.e., a CP even observable) about $\arg(\mu) = 180^\circ$, with ξ neglected as in the analysis of Fig. 4. The polarization asymmetries have strong sensitivities to the μ phase. Note that due to $\tan\beta \lesssim 20$, the μ phase has effects on both the Higgs scalar–pseudoscalar mixing and the chargino triangle loops (i.e., H_2 may be a mixed state of the CP even and CP odd Higgs bosons), but the M_2 phase influences the triangle diagram alone (i.e., H_2 is almost the pure CP odd state A). This may explain the differences between Figs. 8 and 11.

4.5 Case V: fixed μ and M_2 phases, and the unknown A_t phase

The most general case will be that all the parameters μ, M_2 and A_t are complex numbers. It would not be very illuminating to vary all the parameters simultaneously. Once the ILC starts to run, one can determine μ and M_2 (both the moduli and phases) and also $\tan\beta$ without ambiguities from $e^+e^- \to \chi_i^+\chi_j^-$. Then the only unknown phase will be contained in the A_t parameter. Therefore, in this subsection, it is assumed that two complex parameters μ and M_2 are completely known from the ILC. Specifically, we fix $\arg(\mu) = \arg(M_2) = 45^\circ$ and vary $\arg(A_t)$ from 0° to 360° for the parameter set (22).

In Fig. 12, the cross sections for $\gamma\gamma \to H_{2,3}$ are presented as functions of $\arg(A_t)$ for $\tan\beta = 10$. In Fig. 13, the cross sections for $\gamma\gamma \to H_{i=1,2,3}$ are shown as functions of M_{H_i}. In Fig. 14, we show the asymmetries $\mathcal{A}_a(H_2)$ (left) and $\mathcal{A}_a(H_3)$ (right) as functions of $\arg(A_t)$. Note that there is no more symmetry around $\arg(A_t) = 180^\circ$ for the nonzero μ and M_2 phases in Figs. 12 and 14. The structures are richer and more complicated than the previous cases.

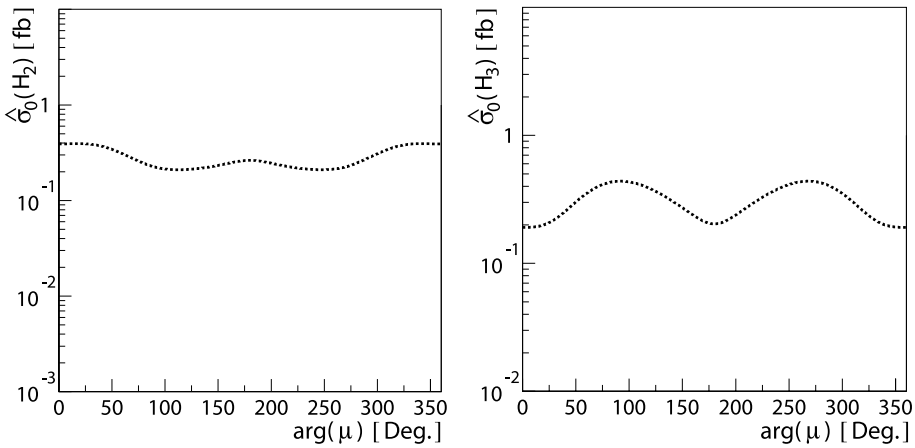

Fig. 9. In Case IV, the cross sections for $\gamma\gamma \to H_2$ (*left*) and $\gamma\gamma \to H_3$ (*right*) in units of fb as functions of $\arg(\mu)$. We choose $M_{H^+} = 300\,\text{GeV}$ and $\arg(A_t) = \arg(M_2) = 0^\circ$ for the parameter set (22)

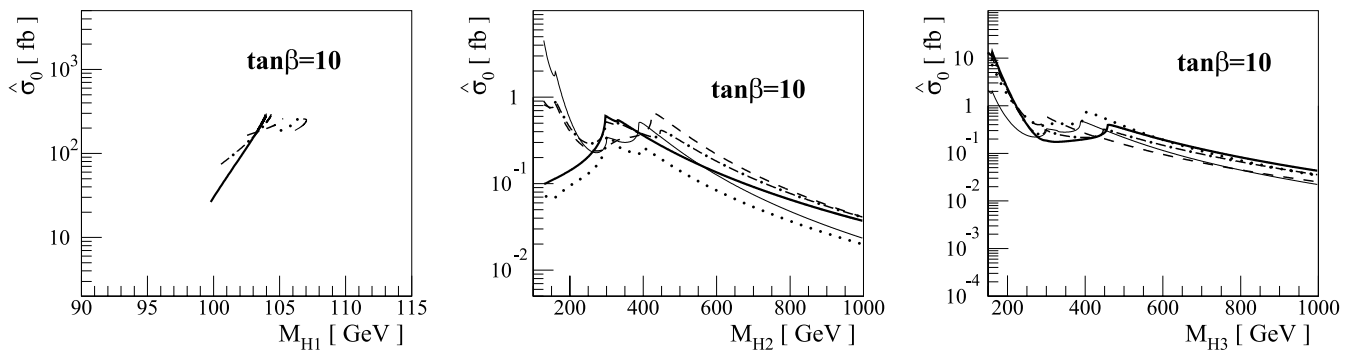

Fig. 10. In Case IV, the unpolarized cross sections for $\gamma\gamma \to H_i$ $(i = 1, 2, 3)$ for $M_2 = 150\,\text{GeV}$ in units of fb as functions of each Higgs mass for five different values of the μ phase: $\arg(\mu) = 0^\circ$ (*thick solid curve*), 40° (*dash-dotted curve*), 80° (*dashed curve*), 120° (*dotted curve*) and 160° (*solid curve*). The phases of M_2 and A_t are set to zero

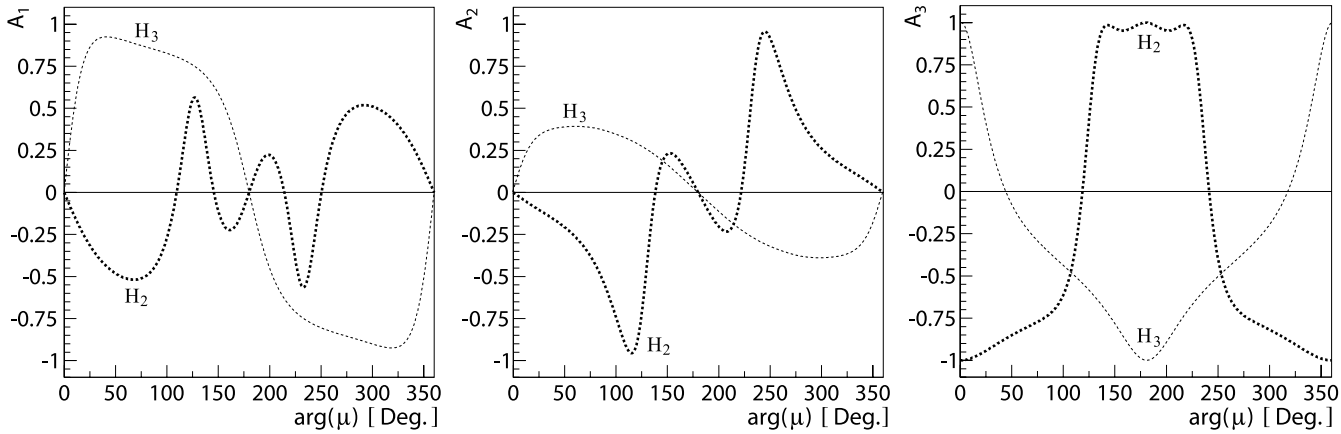

Fig. 11. In Case IV, the polarization asymmetries $\mathcal{A}_a$ $(a = 1, 2, 3)$ of H_2 (*thick dotted curve*) and H_3 (*dotted curve*) with the chargino loop contributions as functions of $\arg(\mu)$. We choose $M_{H^+} = 300\,\text{GeV}$ and $\arg(A_t) = \arg(M_2) = 0^\circ$ for the parameter set (22)

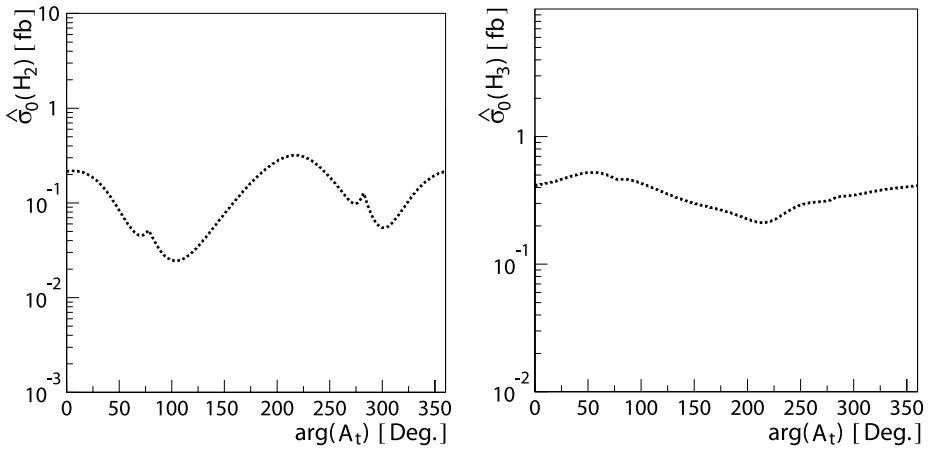

Fig. 12. In Case V, the cross sections for $\gamma\gamma \to H_2$ (*left*) and $\gamma\gamma \to H_3$ (*right*) in units of fb as functions of $\arg(A_t)$. We choose $M_{H^+} = 300\,\text{GeV}$ and $\arg(\mu) = \arg(M_2) = 45^\circ$ for the parameter set (22)

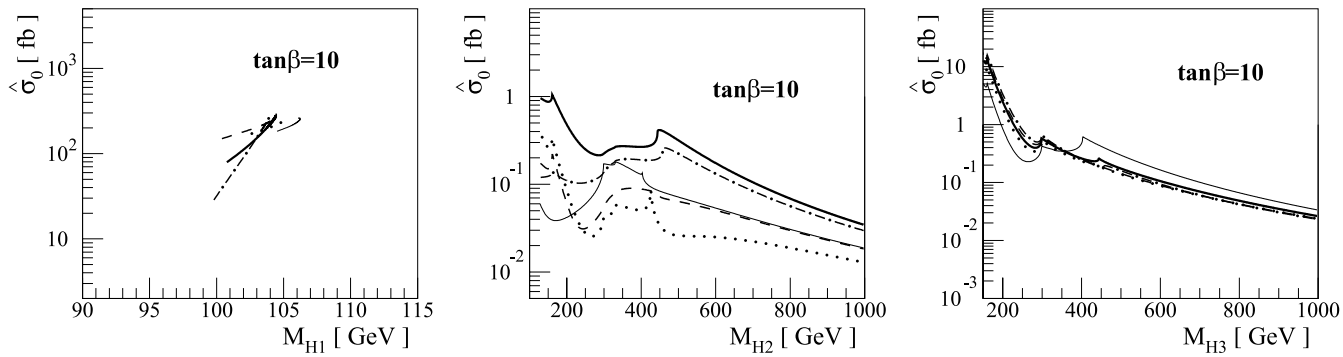

Fig. 13. In Case V, the unpolarized cross sections for $\gamma\gamma \to H_i$ $(i = 1, 2, 3)$ for $M_2 = 150\,\text{GeV}$ in units of fb as functions of each Higgs mass for five different values of the A_t phase: $\arg(A_t) = 0^\circ$ (*thick solid curve*), 40° (*dash-dotted curve*), 80° (*dashed curve*), 120° (*dotted curve*) and 160° (*solid curve*). The phases of M_2 and A_t are set to 45°

Since still the production cross sections for the heavier neutral Higgs bosons are smaller than 1 fb in most parameter space, it would not be easy to produce and study them at photon colliders. However, the production cross section for the lightest neutral Higgs boson H_1 is quite large, and it also depends on the CP phases to some extent – this implies that the lightest neutral Higgs boson could be studied in detail at photon colliders. Note that the determination of the soft SUSY breaking sector involving the stop sector is a phenomenologically important issue. It is not possible to achieve this by utilizing the process $e^+e^- \to \tilde{t}_i\tilde{t}_i^*$ alone. Whether Higgs sector CP violation due to the nonzero A_t

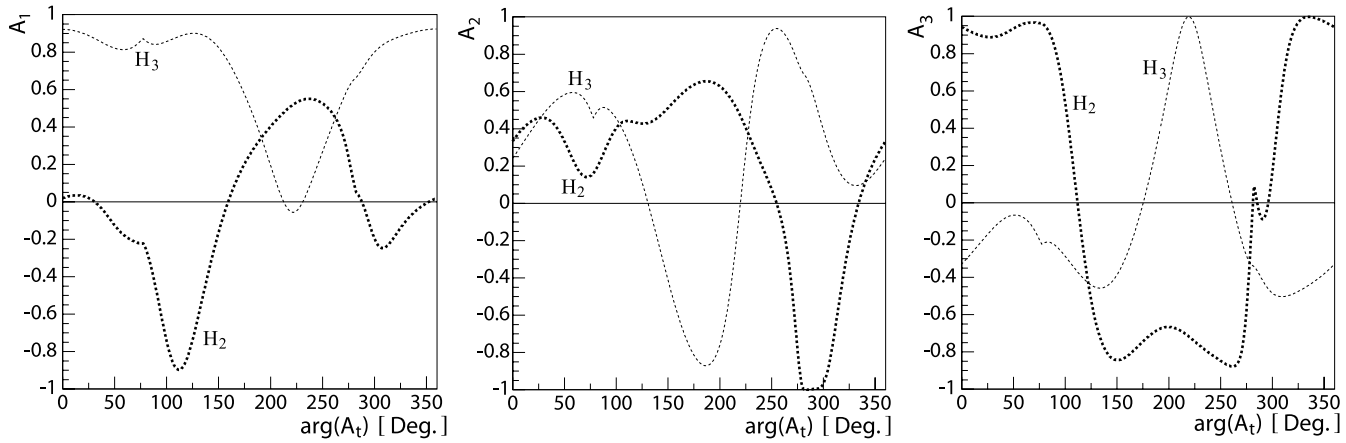

Fig. 14. In Case V, the polarization asymmetries $\mathcal{A}_a$ $(a = 1, 2, 3)$ of H_2 (*thick dotted curve*) and H_3 (*dotted curve*) with the chargino loop contributions as functions of $\arg(A_t)$. We choose $M_{H^+} = 300$ GeV and $\arg(\mu) = \arg(M_2) = 45^\circ$ for the parameter set (22)

phase could be helpful deserves a further careful study, and will be discussed elsewhere.

5 Conclusions

In this work, we presented a comprehensive analysis of neutral Higgs boson production at photon colliders through $\gamma\gamma \to H_{i=1,2,3}$ in the presence of the Higgs sector CP violation of the MSSM. In particular, we have included the chargino loop contributions, which were ignored in the previous studies. In many SUSY breaking scenarios in the literature, charginos are not too heavy, so that their effects are generically important. The production of the would-be CP odd H_2 boson is enhanced by an order of magnitude when chargino loop contributions are included even without Higgs sector CP violation. If the phases of the A_t, M_2 and μ parameters are turned on, the CP violation in the Higgs sector becomes very rich in structure due to the indirect and direct CP violations. This is also true of the case of the heaviest Higgs boson H_3. In addition, the polarization asymmetries are affected by the Higgs sector CP violation. When the parameters A_t, M_2 and μ have large CP violating phases, their effects can appear in various physical observables: e.g., the Higgs sector CP violation as discussed in this work, and also the direct CP violation in $B \to X_s\gamma$ [58–63]. Since the latter is an indirect signature, it is important to probe SUSY CP violation in a direct way. Thus it is important to investigate CP violation from the soft SUSY breaking sector such as $\arg(A_t)$, $\arg(M_2)$ and $\arg(\mu)$ in the Higgs sector CP violation by using $\gamma\gamma$ colliders as discussed in this work. In this regard, the $\gamma\gamma$ mode at ILC with high $\sqrt{s_{\gamma\gamma}}$ and luminosity and high quality beam polarizations will be indispensable for this purpose by measuring the cross sections of $\gamma\gamma \to H_i$ $(i = 1, 2, 3)$ and the three asymmetries $\mathcal{A}_a(H_i)$ $(a = 1, 2, 3)$ in the MSSM. Since the production cross sections for the heavier neutral Higgs bosons are smaller than 1 fb in most of the parameter space, it would be difficult to produce them and study their CP properties at the current planned luminosity at photon colliders. It would be most desirable to increase the luminosity of the photon colliders.

Acknowledgements. We are grateful to S.Y. Choi and Jae Sik Lee for useful communications and to W.Y. Song for discussions. This work was supported in part by KOSEF Sundo grant R02-2003-000-10085-0 and by KOSEF through CHEP at Kyungpook National University.

Appendix A: Charginos and scalar tops

The chargino mass matrix in the $(\tilde{W}^+, \tilde{H}^+)$ basis [55] is

$$\mathcal{M}_C = \begin{pmatrix} M_2 & \sqrt{2}\mathrm{e}^{-\mathrm{i}\xi} m_W \cos\beta \\ \sqrt{2} m_W \sin\beta & \mu \end{pmatrix}, \qquad (A.1)$$

where M_2 and μ are wino and higgsino masses, and $\mathrm{e}^{+\mathrm{i}\xi}$ is the phase of the up-type Higgs VEV [11–13]. Since the mass matrix $\mathcal{M}_C$ is a general complex matrix, it is diagonalized by a biunitary transformation:

$$U^* \mathcal{M}_C V^{-1} \equiv \mathrm{diag}(M_{\tilde{\chi}_1^-}, M_{\tilde{\chi}_2^-}), \qquad (A.2)$$

with $M_{\tilde{\chi}_2^-} \geq M_{\tilde{\chi}_1^-} \geq 0$. In order for $M_{\tilde{\chi}_{i=1,2}^-}$ to be positive, we define the unitary matrix U as a product of two unitary matrices

$$U \equiv H U'. \qquad (A.3)$$

The angles θ_1 and ϕ_1 of the unitary matrix

$$U' = \begin{pmatrix} \cos\frac{\theta_1}{2} & \mathrm{e}^{+\mathrm{i}\phi_1} \sin\frac{\theta_1}{2} \\ -\mathrm{e}^{-\mathrm{i}\phi_1} \sin\frac{\theta_1}{2} & \cos\frac{\theta_1}{2} \end{pmatrix} \qquad (A.4)$$

are given by

$$\tan\theta_1 = \Big\{2\sqrt{2}m_W\big[|M_2|^2\cos^2\beta+|\mu|^2\sin^2\beta + |M_2|\,|\mu|\sin 2\beta\cos(\delta_\mu+\delta_2+\xi)\big]^{1/2}\Big\}\Big/ \big\{|M_2|^2-|\mu|^2-2m_W^2\cos 2\beta\big\}, \quad (A.5)$$

$$\tan\phi_1 = \frac{-|M_2|\sin\delta_2\cos\beta+|\mu|\sin(\delta_\mu+\xi)\sin\beta}{|M_2|\cos\delta_2\cos\beta+|\mu|\cos(\delta_\mu+\xi)\sin\beta}, \quad (A.6)$$

where $\delta_\mu = \arg(\mu)$ and $\delta_2 = \arg(M_2)$. The unitary mixing matrix V is

$$V = \begin{pmatrix} \cos\frac{\theta_2}{2} & \mathrm{e}^{-\mathrm{i}\phi_2}\sin\frac{\theta_2}{2} \\ -\mathrm{e}^{+\mathrm{i}\phi_2}\sin\frac{\theta_2}{2} & \cos\frac{\theta_2}{2}\end{pmatrix} \quad (A.7)$$

where

$$\tan\theta_2 = \Big\{2\sqrt{2}m_W\big[|M_2|^2\sin^2\beta+|\mu|^2\cos^2\beta + |M_2||\mu|\sin 2\beta\cos(\delta_\mu+\delta_2+\xi)\big]^{1/2}\Big\}\Big/ \big\{|M_2|^2-|\mu|^2+2m_W^2\cos 2\beta\big\}, \quad (A.8)$$

$$\tan\phi_2 = \frac{|M_2|\sin(\delta_2+\xi)\sin\beta-|\mu|\sin\delta_\mu\cos\beta}{|M_2|\cos(\delta_2+\xi)\sin\beta+|\mu|\cos\delta_\mu\cos\beta}. \quad (A.9)$$

By using the unitary matrix $H = \mathrm{diag}(\mathrm{e}^{\mathrm{i}\gamma_1}, \mathrm{e}^{\mathrm{i}\gamma_2})$, where $\gamma_{1,2}$ are the phases of the diagonal elements of $U'^*\mathcal{M}_C V^{-1}$, we finally obtain

$$U^*\mathcal{M}_C V^{-1} = \mathrm{diag}(M_{\tilde{\chi}_1^-}, M_{\tilde{\chi}_2^-}). \quad (A.10)$$

And the mass eigenvalues of charginos are

$$M^2_{\tilde{\chi}_1^-,\tilde{\chi}_2^-} = \frac{1}{2}\big(|M_2|^2+|\mu|^2+2m_W^2\big) \mp \frac{1}{2}\big[(|M_2|^2-|\mu|^2)^2 + 4m_W^4\cos^2 2\beta + 4m_W^2\big(|M_2|^2+|\mu|^2 + 2|M_2|\,|\mu|\cos(\delta_\mu+\delta_2)\sin 2\beta\big)\big]^{1/2}. \quad (A.11)$$

Note that the mass eigenvalues and the mixing angles depend on the CP violating phases ξ, δ_μ, and δ_2.

The stop (mass)^2 matrix $\mathcal{M}_{\tilde{t}}^2$ [51] is written as

$$\mathcal{L}^{\mathrm{eff}}_{\mathrm{mass}} = -(\tilde{t}_{\mathrm{L}}^*\ \ \tilde{t}_{\mathrm{R}}^*)\mathcal{M}_{\tilde{t}}^2\begin{pmatrix}\tilde{t}_{\mathrm{L}}\\ \tilde{t}_{\mathrm{R}}\end{pmatrix} = -(\tilde{t}_{\mathrm{L}}^*\ \ \tilde{t}_{\mathrm{R}}^*)\begin{pmatrix} m^2_{\tilde{t}\mathrm{L}} & m^2_{\tilde{t}\mathrm{LR}} \\ m^{2*}_{\tilde{t}\mathrm{LR}} & m^2_{\tilde{t}\mathrm{R}}\end{pmatrix}\begin{pmatrix}\tilde{t}_{\mathrm{L}}\\ \tilde{t}_{\mathrm{R}}\end{pmatrix}, \quad (A.12)$$

where

$$m^2_{\tilde{t}\mathrm{L}} = M^2_{\tilde{t}_{\mathrm{L}}} + m_t^2 + m_Z^2\cos 2\beta\left(\frac{1}{2}-\frac{2}{3}\sin^2\theta_W\right), \quad (A.13)$$

$$m^2_{\tilde{t}\mathrm{R}} = M^2_{\tilde{t}_{\mathrm{R}}} + m_t^2 + m_Z^2\cos 2\beta\cdot\frac{2}{3}\sin^2\theta_W, \quad (A.14)$$

$$m^2_{\tilde{t}\mathrm{LR}} = m_t\big(A_t^*\mathrm{e}^{-\mathrm{i}\xi}-\mu\cot\beta\big). \quad (A.15)$$

The stop mixing angle $\theta_{\tilde{t}}$ is

$$\theta_{\tilde{t}} = \frac{1}{2}\arctan\left(\frac{2\big|m^2_{\tilde{t}\mathrm{LR}}\big|}{m^2_{\tilde{t}\mathrm{L}}-m^2_{\tilde{t}\mathrm{R}}}\right). \quad (A.16)$$

The relations between the mass and the weak eigenstates of stops are given by

$$\tilde{t}_1 = \tilde{t}_{\mathrm{L}}\cos\theta_{\tilde{t}} + \tilde{t}_{\mathrm{R}}\mathrm{e}^{-\mathrm{i}\beta_{\tilde{t}}}\sin\theta_{\tilde{t}},$$
$$\tilde{t}_2 = -\tilde{t}_{\mathrm{L}}\mathrm{e}^{\mathrm{i}\beta_{\tilde{t}}}\sin\theta_{\tilde{t}} + \tilde{t}_{\mathrm{R}}\cos\theta_{\tilde{t}}, \quad (A.17)$$

where $\beta_{\tilde{t}} = -\arg(m^2_{\tilde{t}\mathrm{LR}})$. The mass eigenvalues of the lighter and heavier stops are

$$m^2_{\tilde{t}_1,\tilde{t}_2} = \frac{1}{2}\Big(m^2_{\tilde{t}\mathrm{L}}+m^2_{\tilde{t}\mathrm{R}} \mp \sqrt{\big(m^2_{\tilde{t}\mathrm{L}}-m^2_{\tilde{t}\mathrm{R}}\big)^2+4\big|m^2_{\tilde{t}\mathrm{LR}}\big|^2}\Big). \quad (A.18)$$

Note that $m^2_{\tilde{t}_1,\tilde{t}_2}$ is dependent on the CP violating phases $\arg(A_t)$ and $\arg(\mu)$ due to $m^2_{\tilde{t}\mathrm{LR}}$ in (A.15).

Appendix B: Relevant couplings

In this section, we list the couplings relevant to $\gamma\gamma\to H_i$ $(i=1,2,3)$ that appear in Table 1.

- The Higgs–fermion–fermion couplings:

$$\mathcal{L}_{H\bar{f}f} = -\frac{gm_f}{2m_W}\bar{f}\left[\left(\frac{v_f^i}{R_\beta^f}\right)-\mathrm{i}\gamma_5\left(\frac{\bar{R}_\beta^i a_f^i}{R_\beta^f}\right)\right]fH_i, \quad (B.1)$$

where

$$R_\beta^d = \bar{R}_\beta^u = \cos\beta\equiv c_\beta, \qquad R_\beta^u = \bar{R}_\beta^d = \sin\beta\equiv s_\beta,$$
$$v_f^d = O_{1,i}, \quad v_f^u = O_{2,i}, \qquad a_f^d = a_f^u = O_{3,i}. \quad (B.2)$$

Here the matrix O diagonalizes the Higgs mass matrix as in (5). In the presence of Higgs sector CP violation, the Higgs bosons couple with both CP even and CP odd bilinears, $\bar{f}f$ and $\bar{f}\gamma_5 f$, simultaneously.

- The Higgs–W–W couplings are determined by the gauge couplings:

$$\mathcal{L}_{HW^+W^-} = gm_W(c_\beta O_{1,i}+s_\beta O_{2,i})H_iW_\mu^+W^{-\mu}. \quad (B.3)$$

- The Higgs–sfermion–sfermion couplings:

$$\mathcal{L}_{H_i\tilde{f}_j\tilde{f}_k} = g^i_{\tilde{f}_j\tilde{f}_k}\tilde{f}_j^*\tilde{f}_kH_i, \quad (B.4)$$

where

$$g^i_{\tilde{f}_j\tilde{f}_k} = \tilde{C}^f_{\alpha;\beta\gamma}O_{\alpha,i}(U_f)^*_{\beta j}(U_f)_{\gamma k}. \quad (B.5)$$

The matrix U_f diagonalizes the sfermion mass matrix

$$U_f^\dagger M_{\tilde{f}}^2 U_f = \mathrm{diag}\left(m^2_{\tilde{f}_1}, m^2_{\tilde{f}_2}\right), \quad (B.6)$$

where $m_{\tilde{f}_1} \leq m_{\tilde{f}_2}$. The indices α and $\{\beta, \gamma\}$ label the three neutral Higgs bosons (ϕ_1, ϕ_2, a) and the sfermion chiralities $\{L, R\}$, respectively. The explicit expressions for $\tilde{C}^f_{\alpha;\beta\gamma}$ can be found in [64].

- The H_i–H^+–H^- couplings are determined by the Higgs potential. If we define

$$\mathcal{L}_{H_i H^+ H^-} = v C_i H_i H^+ H^- \,, \tag{B.7}$$

then the couplings C_i are given by [43, 44]

$$C_i = \sum_{\alpha=1,2,3} O_{\alpha,i} c_\alpha \,, \tag{B.8}$$

with

$$\begin{aligned}
c_1 &= 2 s_\beta^2 c_\beta \lambda_1 + c_\beta^3 \lambda_3 - s_\beta^2 c_\beta \lambda_4 - 2 s_\beta^2 c_\beta \,\mathrm{Re}\left(\lambda_5 \mathrm{e}^{2\mathrm{i}\xi}\right) \\
&\quad + s_\beta \left(s_\beta^2 - 2 c_\beta^2\right) \mathrm{Re}\left(\lambda_6 \mathrm{e}^{\mathrm{i}\xi}\right) + s_\beta c_\beta^2 \,\mathrm{Re}\left(\lambda_7 \mathrm{e}^{\mathrm{i}\xi}\right) , \\
c_2 &= 2 c_\beta^2 s_\beta \lambda_2 + s_\beta^3 \lambda_3 - c_\beta^2 s_\beta \lambda_4 - 2 c_\beta^2 s_\beta \,\mathrm{Re}\left(\lambda_5 \mathrm{e}^{2\mathrm{i}\xi}\right) \\
&\quad + c_\beta s_\beta^2 \,\mathrm{Re}\left(\lambda_6 \mathrm{e}^{\mathrm{i}\xi}\right) + c_\beta \left(c_\beta^2 - 2 s_\beta^2\right) \mathrm{Re}\left(\lambda_7 \mathrm{e}^{\mathrm{i}\xi}\right) , \\
c_3 &= 2 s_\beta c_\beta \,\mathrm{Im}\left(\lambda_5 \mathrm{e}^{2\mathrm{i}\xi}\right) - s_\beta^2 \,\mathrm{Im}\left(\lambda_6 \mathrm{e}^{\mathrm{i}\xi}\right) - c_\beta^2 \,\mathrm{Im}\left(\lambda_7 \mathrm{e}^{\mathrm{i}\xi}\right) .
\end{aligned} \tag{B.9}$$

References

1. J.F. Gunion, H.E. Haber, G. Kane, S. Dawson, The Higgs Hunter's Guide (Addison-Wesley, Redwood City, 1990)
2. N. Maekawa, Phys. Lett. B **282**, 387 (1992)
3. A. Pomarol, Phys. Lett. B **287**, 331 (1992)
4. N. Haba, Phys. Lett. B **398**, 305 (1997)
5. O.C.W. Kong, F.-L. Lin, Phys. Lett. B **419**, 217 (1998)
6. S. Baek, P. Ko, Phys. Lett. B **462**, 95 (1999)
7. M. Carena, M. Quiros, C.E.M. Wagner, Phys. Lett. B **380**, 81 (1996)
8. M. Carena, M. Quiros, C.E.M. Wagner, Nucl. Phys. B **524**, 3 (1998)
9. J.M. Cline, K. Kainulainen, Nucl. Phys. B **482**, 73 (1996)
10. J.M. Cline, G.D. Moore, Phys. Rev. Lett. **81**, 3315 (1998)
11. A. Pilaftsis, C.E.M. Wagner, Nucl. Phys. B **553**, 3 (1999)
12. S.Y. Choi, M. Drees, J.S. Lee, Phys. Lett. B **481**, 57 (2000)
13. M. Carena, J. Ellis, A. Pilaftsis, C.E.M. Wagner, Nucl. Phys. B **586**, 92 (2000)
14. S. Dimopoulos, G.F. Giudice, Phys. Lett. B **357**, 573 (1995)
15. A. Cohen, D.B. Kaplan, A.E. Nelson, Phys. Lett. B **388**, 599 (1996)
16. A. Pomarol, D. Tommasini, Nucl. Phys. B **488**, 3 (1996)
17. P. Binétruy, E. Duda, Phys. Lett. B **389**, 503 (1996)
18. T. Ibrahim, P. Nath, Phys. Lett. B **418**, 98 (1998)
19. T. Ibrahim, Phys. Rev. D **57**, 478 (1998)
20. T. Ibrahim, P. Nath, Phys. Rev. D **58**, 019 901 (1998)
21. T. Ibrahim, P. Nath, Phys. Rev. D **58**, 111 301 (1998)
22. T. Falk, K.A. Olive, M. Pospelov, R. Roiban, Nucl. Phys. B **560**, 3 (1999)
23. S. Abel, S. Khalil, O. Lebedev, Nucl. Phys. B **606**, 151 (2000)
24. D. Chang, W.-Y. Keung, A. Pilaftsis, Phys. Rev. Lett. **82**, 900 (1999)
25. J.F. Gunion, H.E. Haber, Phys. Rev. D **48**, 5109 (1993)
26. D.L. Borden, D.A. Bauer, D.O. Caldwell, Phys. Rev. D **48**, 4018 (1993)
27. D. Grzadkowski, J.F. Gunion, Phys. Lett. B **294**, 361 (1992)
28. M. Krämer, J. Kühn, M.L. Stong, P.M. Zerwas, Z. Phys. C **64**, 21 (1994)
29. H.F. Ginzburg, G.L. Kotkin, V.G. Serbo, V.I. Telnov, Nucl. Instrum. Methods **205**, 47 (1983)
30. H.F. Ginzburg, G.L. Kotkin, S.L. Panfil, V.G. Serbo, V.I. Telnov, Nucl. Instrum. Methods **219**, 5 (1984)
31. T.L. Barklow, in: Research Directions for the Decade, Proc. of the Summer Study on High Energy Physics, Snowmass, Colorado, 1990, ed. by E.L. Berger (World Scientific, Singapore, 1991) p. 440
32. D.L. Borden, D.A. Bauer, D.O. Caldwell, SLAC Report No. SLAC-PUB-5715, 1992 (unpublished)
33. J.S. Lee, Mod. Phys. Lett. A **22**, 1191 (2007)
34. R.M. Godbole, S.D. Rindani, R.K. Singh, Phys. Rev. D **67**, 095 009 (2003)
35. J.R. Ellis, J.S. Lee, A. Pilaftsis, Nucl. Phys. B **718**, 247 (2005)
36. R.M. Godbole, S. Kraml, S.D. Rindani, R.K. Singh, Phys. Rev. D **74**, 095 006 (2006)
37. M. Carena, S. Heinemeyer, C.E.M. Wagner, G. Weiglein, Eur. Phys. J. C **45**, 797 (2006)
38. J. Ellis, J.S. Lee, A. Pilaftsis, Mod. Phys. Lett. A **21**, 1405 (2006)
39. J. Ellis, J.S. Lee, A. Pilaftsis, Phys. Rev. D **71**, 075007 (2005)
40. D.K. Ghosh, S. Moretti, Eur. Phys. J. C **42**, 341 (2005)
41. G. Ferrera, B. Mele, Eur. Phys. J. C **42**, 425 (2005)
42. M. Carena, J. Ellis, S. Mrenna, A. Pilaftsis, C.E.M. Wagner, Nucl. Phys. B **659**, 145 (2003)
43. S.Y. Choi, J.S. Lee, Phys. Rev. D **62**, 036 005 (2000)
44. J.S. Lee, Proc. "Theory Meeting on Physics at Linear Colliders", KEK, Japan, 2001 [hep-ph/0106327]
45. M.A. Diaz, S.F. King, Phys. Lett. B **373**, 100 (1996)
46. ALEPH, DELPHI, L3, OPAL Collaborations, Eur. Phys. J. C **47**, 547 (2006)
47. A. Pilaftsis, Phys. Rev. D **58**, 096 010 (1998)
48. A. Pilaftsis, Phys. Lett. B **435**, 88 (1998)
49. T. Ibrahim, P. Nath, Phys. Rev. D **63**, 035 009 (2001)
50. M. Carena, J.R. Espinosa, M. Quirós, C.E.M. Wagner, Phys. Lett. B **355**, 209 (1995)
51. S. Bae, Phys. Lett. B **489**, 171 (2000)
52. A. Dedes, S. Moretti, Phys. Rev. Lett. **84**, 22 (2000)
53. S.Y. Choi, J.S. Lee, Phys. Rev. D **61**, 115 002 (2000)
54. S.Y. Choi, K. Hagiwara, J.S. Lee, Phys. Lett. B **529**, 212 (2002)
55. H.E. Haber, G.L. Kane, Phys. Rep. **117**, 75 (1985)
56. T. Takahasi, Nucl. Instrum. Methods A **472**, 4 (2001)
57. V. Telnov, Nucl. Instrum. Methods A **472**, 43 (2001)
58. S. Baek, P. Ko, Phys. Rev. Lett. **83**, 488 (1999)
59. T. Goto, Y.Y. Keum, T. Nihei, Y. Okada, Y. Shimizu, Phys. Lett. B **460**, 333 (1999)
60. M. Aoki, G.-C. Cho, N. Oshimo, Phys. Rev. D **60**, 035 004 (1999)
61. D. Bailin, S. Khalil, Phys. Rev. Lett. **86**, 4227 (2001)
62. D.A. Demir, K.A. Olive, Phys. Rev. D **65**, 034 007 (2002)
63. H. Murayama, A. Pierce, Phys. Rev. D **67**, 071 702 (2003)
64. S.Y. Choi, J.S. Lee, Phys. Rev. D **61**, 115 002 (2000)